SIAM J. Applied Dynamical Systems
Vol. 21, No. 2, pp. 932–959

Stochastically Adaptive Control and Synchronization: From Globally One-Sided Lipschitzian to Only Locally Lipschitzian Systems*

Shijie Zhou†, Ying-Cheng Lai‡, and Wei Lin§

Abstract. The mathematical framework of stochastically adaptive feedback control, which is generally applicable to significant problems in nonlinear dynamics such as stabilization and synchronization, has been previously established but only for systems whose vector fields satisfy the global Lipschitzian condition. Nonlinear dynamical systems arising from physical, chemical, or biological situations are typically described by vector fields that are only locally Lipschitzian. To generalize the mathematical theory of stochastically adaptive control to realistic systems is quite a challenging and formidable task. We meet this challenge by proving rigorously that stabilization and synchronization can be achieved with probability one for only locally Lipschitzian systems. The result holds not only for one-dimensional but also for any finite-dimensional white noises. Representative examples and an application to synchronization-based parameter identification are presented to illustrate the broad applicability of the developed mathematical criteria. Our successful relaxation of the mathematical condition from globally to locally Lipschitzian provides a rigorous guarantee of the stability of stochastically adaptive control in physical systems with significant implications to the design and realization of engineering control systems.

Key words. stochastically adaptive feedback control, locally Lipschitzian system, control stability, synchronization, parameter identification

AMS subject classifications. 60H10, 34F05, 93E99

DOI. 10.1137/21M1402042

1. Introduction.

In the study of nonlinear dynamical systems from the physical world, the ultimate goal is to be able to control them. In the design and development of engineering systems, the problem of control is fundamental. For nonlinear dynamical systems, existing control methodologies can be classified into two: open-loop [48, 15, 7] and closed-loop control [55, 56, 27, 2, 66, 13]. A closely related problem is synchronization [51], which

*Received by the editors March 2, 2021; accepted for publication (in revised form) by I. Belykh December 1, 2021; published electronically April 13, 2022.
https://doi.org/10.1137/21M1402042
Funding: This work was supported by the MOE Frontiers Center for Brain Science, LMNS, and LCNBI, Fudan University, China, by NSF of China grants 61773125 and 11925103, and by Science and Technology Commission of Shanghai Municipality grants 19511101404, 19511132000, and 2021SHZDZX0103. The work at Arizona State University was supported by the Army Research Office through grant W911NF-21-2-0055 and by the Air Force Office of Scientific Research through grant FA9550-21-1-0438.
†School of Mathematical Sciences, Shanghai Center for Mathematical Science, and Research Institute of Intelligent Complex Systems, Fudan University, Shanghai 200433, China, and Department of Mathematics and Statistics, York University, Toronto, Canada (sjzhou14@fudan.edu.cn).
‡School of Electrical, Computer and Energy Engineering, Arizona State University, Tempe, AZ 85281 USA (Ying-Cheng.Lai@asu.edu).
§Corresponding author. School of Mathematical Sciences, Shanghai Center for Mathematical Science, Research Institute of Intelligent Complex Systems, and Centre for Systems Computational Biology of ISTBI, Fudan University, Shanghai 200433, China (wlin@fudan.edu.cn).

can be formulated as a problem of open-loop control for chaotic systems [33, 46] and networks [6, 52, 9, 86], closed-loop control [4, 3, 28, 57, 84, 58, 32, 83, 85, 10], or pinning control (a special type of closed-loop control) [16, 71, 82, 76, 80]. Associated with feedback closed-loop control, adaptive schemes to enhance the control feasibility have been investigated [27, 8, 82, 35, 65, 40, 64, 67, 84]. Previous studies have also revealed interestingly that stochastic disturbances, noise, or temporal switches can induce stability and synchronization [4, 42, 44, 3, 28, 75, 74, 21, 20, 19, 58, 32, 23, 24, 63, 29, 14, 22].

This paper deals with the problem of stochastically adaptive control of nonlinear dynamical systems. Mathematically, the formulation of the problem begins with the setting

$$\mathrm{d}\boldsymbol{x}_t = \boldsymbol{f}(\boldsymbol{x}_t)\mathrm{d}t + \sum_{l=1}^{m} \boldsymbol{A}_l \boldsymbol{x}_t \mathrm{d}B_l(t), \tag{1.1}$$

where $\boldsymbol{x}_t \in \mathbb{R}^p$ is a state variable with $t \geq 0$, $\boldsymbol{f} : \mathbb{R}^p \to \mathbb{R}^p$ is the vector field with $\boldsymbol{f}(\boldsymbol{0}) = \boldsymbol{0}$, the control target is $\boldsymbol{x}_t \equiv \boldsymbol{0}$, and $\boldsymbol{B}(t) = \big[B_1(t), B_2(t), \ldots, B_m(t)\big]^\top$ denotes a standard m-dimensional Brownian process. In order to realize stabilization, $\boldsymbol{A}_l \in \mathbb{R}^{p\times p}$ $(l = 1, 2, \ldots, m)$ should be *a* priori specified constant feedback matrices that depend on the explicit form of the system (1.1). In realistic applications, information about the underlying system may be incomplete, motivating the introduction of appropriately designed adaptive schemes in which the matrices $\boldsymbol{A}_l$ are adjusted in time according to the state of the system. A recently studied stochastically adaptive feedback scheme [36] is

$$\mathrm{d}\boldsymbol{x}_t = \boldsymbol{f}(\boldsymbol{x}_t)\mathrm{d}t + k_t \boldsymbol{x}_t \mathrm{d}B(t), \quad \mathrm{d}k_t = \|\boldsymbol{x}_t\|^\theta \mathrm{d}t, \tag{1.2}$$

where $\|\cdot\|$ is the normal Euclidean norm, $B(t)$ represents a one-dimensional Brownian process, and $0 < \theta < 1$ is a parameter. It was proved [36] that stability of the controlled system can be guaranteed almost surely if the vector field $\boldsymbol{f}(\boldsymbol{x}_t)$ satisfies the globally one-sided Lipschitzian condition, i.e., the derivative of each component of the vector field is bounded. While the global Lipschitzian condition enables a rigorous mathematical guarantee of stability to be established, it is a mathematical idealization that cannot be expected to hold for realistic natural systems. In fact, for nonlinear dynamical systems describing physical, chemical, or biological processes, the vector fields typically satisfy at most the *locally* one-sided Lipschitzian condition, e.g., the derivatives of the components of the vector field could be globally unbounded. These include the well-studied, classic, and paradigmatic nonlinear dynamical systems such as the Lorenz system [39], the Rössler oscillator [61], the van der Pol–Duffing oscillator [68], the Hindmarsh–Rose oscillator [25], the FitzHugh–Nagumo neuron [12, 45], the classical predator-prey system [60, 26], and so on. A key question is, given a system that satisfies only the locally one-sided Lipschitzian condition, will the stochastically adaptive feedback control scheme still be effective, especially when the dimension of the Brownian process is greater than one? In particular, under such circumstances, is it still possible to obtain a mathematical guarantee of the stability of the control scheme when the prerequisite $0 < \theta < 1$ is extended? An affirmative answer not only is of mathematical interest but, more importantly, has significant implications to the design and realization of stochastic, nonlinear control systems in engineering for which a mathematical guarantee is a necessary prerequisite.

To establish mathematically the stability of stochastically adaptive feedback control systems only with a locally Lipschitzian vector field presents a great challenge. However, as

we will demonstrate in this paper, by employing a probabilistic description, we are able to prove the stability in the sense of probability one. From a practical standpoint, this means that the stochastically adaptive feedback scheme can be applied to nonlinear physical systems for control and synchronization with guaranteed certainty. In addition to providing mathematical proofs, we demonstrate the power of the scheme using a number of examples. We will also show how the scheme can be exploited for system parameter identification through stochastic synchronization, a problem deemed important in applications of nonlinear dynamics [49, 50, 73, 1, 37, 79, 77, 69, 78, 40, 41].

The rest of this article is structured as follows. Section 2 poses the mathematical problem and describes the model formulation. Section 3 presents our main results, which include descriptions of some extended mathematical conditions and rigorous theorems for ensuring stability and synchronization almost surely. Section 4 gives the detailed proofs of the main theorems. Section 5 provides a number of examples on complex systems and networks demonstrating stability and synchronization as guaranteed by our rigorous mathematical results. Section 6 addresses the applied issue of system parameter identification to illustrate the broad applicability of our analytical criteria. Section 7 presents concluding remarks and future perspectives.

2. Framework of stochastically adaptive feedback control and mathematical conditions. We consider dynamical systems that, when uncontrolled, can be described as $\mathrm{d}\boldsymbol{x}_t = \boldsymbol{f}(\boldsymbol{x}_t)\mathrm{d}t$, where $\boldsymbol{f}(\boldsymbol{x})$ is a vector field that satisfies the locally Lipschitzian condition. In the presence of a stochastically adaptive feedback controller, the system becomes

$$\begin{aligned} \mathrm{d}\boldsymbol{x}_t &= \boldsymbol{f}(\boldsymbol{x}_t)\mathrm{d}t + \sum_{l=1}^{m}(k_t\boldsymbol{A}_l)\boldsymbol{x}_t\mathrm{d}B_l(t), \\ \mathrm{d}k_t &= \|\boldsymbol{x}_t\|^{\theta}\mathrm{d}t, \end{aligned} \tag{2.1}$$

where $k_t \in \mathbb{R}$ is a variable that evolves with time which, when being multiplied by the constant matrix $\boldsymbol{A}_l$, generates a dynamic feedback matrix $k_t\boldsymbol{A}_l$. Compared with the static feedback matrix used in previously studied systems (Equation (1.1)), a time-dependent feedback matrix represents a more general formulation of the control problem. In system (2.1), the parameter $\theta > 0$ is the algebraic power associated with the adaptive rule for dynamically adjusting the value of k_t. The locally and globally Lipschitzian conditions for the vector field $\boldsymbol{f}(\boldsymbol{x})$ of the uncontrolled system can be stated as follows.

Condition 2.1 (locally Lipschitzian condition). For any given positive number n, there exists a positive number K_n such that

$$\|\boldsymbol{f}(\boldsymbol{x}) - \boldsymbol{f}(\boldsymbol{y})\| \le K_n\|\boldsymbol{x} - \boldsymbol{y}\|$$

for any $\boldsymbol{x}, \boldsymbol{y} \in \mathbb{R}^p$ with $\|\boldsymbol{x}\| \le n$ and $\|\boldsymbol{y}\| \le n$.

According to the classical theory of stochastic differential equations [43], the locally Lipschitzian condition is sufficient to ensure the uniqueness and local existence of the solution of system (2.1). The quantity K_n in Condition 2.1 depends on the given number n. For a *globally Lipschitzian* vector field, K_n is independent of the choice of n and therefore becomes a constant.

Condition 2.2 (globally one-sided Lipschitzian condition). There exists a positive number L such that

$$\langle \boldsymbol{x}-\boldsymbol{y}, \boldsymbol{f}(\boldsymbol{x})-\boldsymbol{f}(\boldsymbol{y})\rangle \le L\|\boldsymbol{x}-\boldsymbol{y}\|^2$$

for all $\boldsymbol{x},\boldsymbol{y}\in\mathbb{R}^p$, where $\langle\cdot\rangle$ denotes the inner product in $\mathbb{R}^p$. For $\boldsymbol{f}(\boldsymbol{0})=\boldsymbol{0}$ and if we set $\boldsymbol{y}=\boldsymbol{0}$ in the inequality, this condition becomes the globally one-sided Lipschitzian condition *centered at zero*.

Remark 2.3. Although, for a continuous vector field, Condition 2.2 is not so general as Condition 2.1 for K_n which could be dependent crucially on n, this condition still covers some cases where the globally Lipschitzian condition in a regular sense (i.e., K_n in Condition 2.1 is independent of n's choice) is not satisfied. For example, the one-dimensional vector field $f(x)=x-x^3$ is a typical example, meeting Condition 2.2 but dissatisfying the globally Lipschitzian condition.

The next two conditions define the typical constraints on the constant matrices $\boldsymbol{A}_l$.

Condition 2.4. There exists a positive number γ such that

$$-2\sum_{l=1}^{m}\left(\boldsymbol{x}^\top\boldsymbol{A}_l\boldsymbol{x}\right)^2+\sum_{l=1}^{m}\|\boldsymbol{x}\|^2\|\boldsymbol{A}_l\boldsymbol{x}\|^2\le-2\gamma\|\boldsymbol{x}\|^4 \tag{2.2}$$

for all $\boldsymbol{x}\in\mathbb{R}^p$.

Condition 2.5. There exists a positive number $h>0$ such that

$$(\theta-2)\sum_{l=1}^{m}\left(\boldsymbol{x}^\top\boldsymbol{A}_l\boldsymbol{x}\right)^2+\sum_{l=1}^{m}\|\boldsymbol{x}\|^2\|\boldsymbol{A}_l\boldsymbol{x}\|^2\le-h\|\boldsymbol{x}\|^4 \tag{2.3}$$

for some $\theta\in(0,1)$ and all $\boldsymbol{x}\in\mathbb{R}^p$.

Remark 2.6. A direct estimate reveals that Condition 2.5 implies Condition 2.4. In addition, for any given $\theta>0$, using the Cauchy–Schwarz inequality, we have

$$(\theta-2)\sum_{l=1}^{m}\left(\boldsymbol{x}^\top\boldsymbol{A}_l\boldsymbol{x}\right)^2+\sum_{l=1}^{m}\|\boldsymbol{x}\|^2\|\boldsymbol{A}_l\boldsymbol{x}\|^2\ge(\theta-1)\sum_{l=1}^{m}\left(\boldsymbol{x}^\top\boldsymbol{A}_l\boldsymbol{x}\right)^2,$$

which, if the inequality (2.3) for $\theta>0$ is satisfied, implies $\theta\in(0,1)$. This gives the reason why we introduce a particular range for θ in Condition 2.5 directly.

3. Main results: Stochastic stability and stochastic synchronization.

We state the main results on stochastic stability of systems satisfying only the locally Lipschitzian condition and then extend the results to stochastic synchronization (the proofs of these results will be presented in section 4).

First, we have the result on the unique existence of a nontrivial solution of the controlled system (2.1), a stepping stone for further analysis.

Theorem 3.1. *Assume that Condition 2.1 is valid. Then, for any given initial value $\boldsymbol{x}_0\neq\boldsymbol{0}$, there exists a unique, continuously adapted solution $\boldsymbol{x}_t$ of (2.1) almost surely before it tends to zero or diverges in finite time.*

Based on the uniqueness theorem [43], the following result guarantees the effectiveness of the stochastically adaptive feedback controller as defined in system (2.1).

Theorem 3.2. *Assume that Condition 2.1, Condition 2.2 centered at zero, and Condition 2.4 all hold. Then, for any nonzero initial state* $\boldsymbol{x}_0$ *and* $k_0 = 0$*, the controlled trajectory* $\boldsymbol{x}_t$ *in system (2.1) exists on the entire interval* $[0, +\infty)$ *almost surely and it does not approach zero in a finite time duration almost surely. Furthermore, the stochastically adaptive feedback controller is effective for stabilization of system (2.1) in the sense of probability one:* $\lim_{t\to+\infty} \boldsymbol{x}_t = \mathbf{0}$ *almost surely and* $\lim_{t\to+\infty} k_t < +\infty$ *almost surely.*

Remark 3.3. For realization of stochastic stabilization, the prerequisite $0 < \theta < 1$ is no longer required. However, the globally one-sided Lipschitzian condition is still necessary. Additionally, the dimension of the Brownian process can be arbitrarily large, but the constraints on $\boldsymbol{A}_l$ should be taken into account.

The globally one-sided Lipschitzian Condition 2.2 used in Theorem 3.2 can be relaxed to some extent, but not the prerequisite $0 < \theta < 1$. In fact, there is a trade-off between the prerequisite for θ and the Lipschitzian condition on the vector field $\boldsymbol{f}$. The following theorem clarifies this situation.

Theorem 3.4. *Assume that both Condition 2.1 and Condition 2.5 hold. Also assume that the Lipschitzian constant* K_n *specified in Condition 2.1 satisfies*

$$\lim_{n\to+\infty} \frac{K_n^{3/2}}{n^{\theta}} = 0, \tag{3.1}$$

where $\theta \in (0, 1)$ *is specified in Condition 2.5. Then, the stochastically adaptive feedback controller is effective for stabilization of system (2.1) in the sense of probability one.*

Corollary 3.5. *Assume that both Condition 2.1 and Condition 2.5 hold. In addition, assume*

$$\limsup_{\|\boldsymbol{x}\|\to+\infty} \frac{\langle \boldsymbol{x}, \boldsymbol{f}(\boldsymbol{x})\rangle}{\|\boldsymbol{x}\|^{2+\frac{2\theta}{3}}} \le 0, \tag{3.2}$$

where $\theta \in (0, 1)$ *is specified in Condition 2.5. Then, the stochastically adaptive feedback controller is effective for stabilization of system (2.1) in the sense of probability one.*

Remark 3.6. Corollary 3.5 provides a verifiable criterion (3.2) for the vector field $\boldsymbol{f}$ to ensure the condition (3.1) of Theorem 3.4. Under such a condition, the vector field is no longer required to be globally one-sided Lipschitzian: it can be locally Lipschitzian and convergent/divergent in a manner as circumscribed by the criterion (3.2). This represents our main result. The use and power of these mathematical results will be demonstrated in the next section with a number of examples.

As will be described immediately below, the problem of synchronization can be regarded as a particular case of the control problem. Thus, in light of the analytical results above, we have the following results on the realization of stochastic synchronization in unidirectionally, stochastically, and adaptively coupled systems. In particular, the dynamical system

$$\mathrm{d}\boldsymbol{x}_t = \boldsymbol{f}(\boldsymbol{x}_t)\mathrm{d}t \tag{3.3}$$

can be regarded as a driving system with its trajectory $\boldsymbol{x}_t$ uniformly bounded on the entire interval $[0, +\infty)$. A stochastically and adaptively coupled response system can be written as

$$\mathrm{d}\boldsymbol{y}_t = \boldsymbol{f}(\boldsymbol{y}_t)\mathrm{d}t + \sum_{l=1}^{m}(k_t\boldsymbol{A}_l)(\boldsymbol{y}_t - \boldsymbol{x}_t)\mathrm{d}B_l(t), \quad \mathrm{d}k_t = \|\boldsymbol{y}_t - \boldsymbol{x}_t\|^\theta \mathrm{d}t, \tag{3.4}$$

where $\boldsymbol{y}_t \in \mathbb{R}^p$ is the state variable of the response system. The vector field, the Brownian process and the parameters are defined in the same manner as those used in system (2.1). Our aim is to verify that such a lead-follower configuration can ensure the stochastic stability of the synchronization manifold $\boldsymbol{y}_t = \boldsymbol{x}_t$ in the sense of probability one.

Theorem 3.7. *Assume that both Condition 2.2 and Condition 2.4, respectively, on the vector field $\boldsymbol{f}$ and matrix $\boldsymbol{A}_l$ in the coupled systems (3.3) and (3.4) hold. Then, for any initial condition $\boldsymbol{y}_0 \neq \boldsymbol{x}_0$ and $k_0 = 0$, the response trajectory $\boldsymbol{y}_t$ of system (3.4) exists on the entire interval $[0, +\infty)$ and approaches the driving trajectory $\boldsymbol{x}_t$ of system (3.3) in any finite time almost surely. Furthermore, the synchronization manifold possesses the stochastic stability: $\lim_{t\to+\infty}\|\boldsymbol{y}_t - \boldsymbol{x}_t\| = 0$ almost surely with $\lim_{t\to+\infty} k_t < +\infty$ almost surely.*

4. Proofs of the main theorems. We present the detailed proofs of the theorems listed in section 3. The following notations are helpful. Let $(\Omega, \mathscr{F}, \{\mathscr{F}_t\}_{t\geq 0}, \mathbb{P})$ denote the complete probability space with a filtration $\mathscr{F}_t$ satisfying the usual conditions, i.e., it is increasing and right continuous while $\mathscr{F}_0$ contains all $\mathbb{P}$-null sets. The m-dimensional Brownian process $\boldsymbol{B}(t)$ in system (2.1) or (3.4) can then be defined on the probability space $(\Omega, \mathscr{F}, \{\mathscr{F}_t\}_{t\geq 0}, \mathbb{P})$. Let the stopping times be

$$\sigma_n \triangleq \inf\left\{t \geq 0 : \|\boldsymbol{x}_t\| \geq n\right\} \quad \text{and} \quad \zeta_\epsilon \triangleq \inf\left\{t \geq 0 : \|\boldsymbol{x}_t\| \leq \epsilon\right\},$$

respectively, for a sufficiently large positive number n and a small positive number ϵ. Taking the limits of the stopping time series, we can define the explosion time σ_∞ and the time approaching zero, ζ_0, respectively, as $\sigma_\infty \triangleq \lim_{n\to+\infty}\sigma_n$ and $\zeta_0 \triangleq \lim_{\epsilon\to 0+}\zeta_\epsilon$.

Proof of Theorem 3.1. Under the locally Lipschitzian Condition 2.1, the uniqueness and existence of solutions of the stochastic differential equation [81, 87, 53] guarantees the existence of a unique adaptive continuous process $\boldsymbol{x}_t$ such that for any large number n and a small number ϵ, the process with stopping times satisfies

$$\boldsymbol{x}_{t\wedge\tau_n\wedge\zeta_\epsilon} = \boldsymbol{x}_0 + \int_0^{t\wedge\tau_n\wedge\zeta_\epsilon}\boldsymbol{f}(\boldsymbol{x}_s)\mathrm{d}s + \int_0^{t\wedge\tau_n\wedge\zeta_\epsilon}\sum_{l=1}^{m}(k_s\boldsymbol{A}_l)\boldsymbol{x}_s\mathrm{d}B_l(s)$$

and

$$k_{t\wedge\tau_n\wedge\zeta_\epsilon} = \int_0^{t\wedge\tau_n\wedge\zeta_\epsilon}\|\boldsymbol{x}_s\|^\theta\mathrm{d}s.$$

Letting $n \to +\infty$ and $\epsilon \to 0+$ gives that the stochastic process $\boldsymbol{x}_t$ satisfies system (2.1) for $t < \sigma_\infty \wedge \zeta_0$, which completes the proof of Theorem 3.1. ∎

Proof of Theorem 3.2. We divide the proof into several steps. First, we verify that the controlled trajectory $\boldsymbol{x}_t$ of system (2.1) does not approach zero almost certainly before it diverges. For given positive numbers n and ϵ, we apply Itô's formula [38] to $\log(\|\boldsymbol{x}_t\|)$ on the time interval $[0, \sigma_n \wedge \zeta_\epsilon \wedge t]$ to get

$$\begin{aligned}\log(\|\boldsymbol{x}_{\sigma_n\wedge\zeta_\epsilon\wedge t}\|) = \log(\|\boldsymbol{x}_0\|) + \int_0^{\sigma_n\wedge\zeta_\epsilon\wedge t} \frac{1}{2}\|\boldsymbol{x}_s\|^{-4}\Big\{2\big\langle \boldsymbol{x}_s, \boldsymbol{f}(\boldsymbol{x}_s)\big\rangle\|\boldsymbol{x}_s\|^2 \\ + k_s^2\Big[-2\sum_{l=1}^m \Big(\boldsymbol{x}_s^\top \boldsymbol{A}_l\boldsymbol{x}_s\Big)^2 + \sum_{l=1}^m \|\boldsymbol{x}_s\|^2\|\boldsymbol{A}_l\boldsymbol{x}_s\|^2\Big]\Big\}\mathrm{d}s \\ + \sum_{l=1}^m \int_0^{\sigma_n\wedge\zeta_\epsilon\wedge t} k_s\|\boldsymbol{x}_s\|^{-2}\big\langle \boldsymbol{x}_s, \boldsymbol{A}_l\boldsymbol{x}_s\big\rangle \mathrm{d}B_l(s).\end{aligned} \tag{4.1}$$

To estimate the expectation values of the quantities in this integral equation, we need to obtain the estimates of a number of relevant quantities. For a given fixed number T, we have

$$k_t = \int_0^t \|\boldsymbol{x}_s\|^\theta \mathrm{d}s \le n^\theta T$$

for any $t < \sigma_n \wedge T$. We also have a sufficiently large and positive number ν satisfying

$$-2\sum_{l=1}^m \Big(\boldsymbol{x}^\top \boldsymbol{A}_l\boldsymbol{x}\Big)^2 + \sum_{l=1}^m \|\boldsymbol{x}\|^2\|\boldsymbol{A}_l\boldsymbol{x}\|^2 \ge -\nu\|\boldsymbol{x}\|^4,$$

which is different from the estimated upper bound used in Condition 2.4. In addition, on the time interval $[0, \sigma_n \wedge T]$, using Condition 2.1 with $\boldsymbol{y} = 0$ yields $\|\boldsymbol{f}(\boldsymbol{x})\| \le K_n\|\boldsymbol{x}\|$. Using the Cauchy–Schwartz inequality [70], we get

$$\big|\big\langle \boldsymbol{x}, \boldsymbol{f}(\boldsymbol{x})\big\rangle\big| \le \|\boldsymbol{x}\| \cdot \|\boldsymbol{f}(\boldsymbol{x})\| \le K_n\|\boldsymbol{x}\|^2. \tag{4.2}$$

Combining these estimates, we have

$$\begin{aligned}\frac{1}{2}\|\boldsymbol{x}_s\|^{-4}\Big\{2\big\langle \boldsymbol{x}_s, \boldsymbol{f}(\boldsymbol{x}_s)\big\rangle\|\boldsymbol{x}_s\|^2 + k_s^2\Big[-2\sum_{l=1}^m \Big(\boldsymbol{x}_s^\top \boldsymbol{A}_l\boldsymbol{x}_s\Big)^2 + \sum_{l=1}^m \|\boldsymbol{x}_s\|^2\|\boldsymbol{A}_l\boldsymbol{x}_s\|^2\Big]\Big\} \\ \ge -\frac{2K_n + \nu n^{2\theta}T^2}{2}.\end{aligned} \tag{4.3}$$

Following the optional stopping theorem [38], we have that the last term on the right side of (4.1) is a martingale on the interval $[0, T]$. Consequently, by taking the expectation values on both sides of (4.1) and using the estimate in (4.3) together with the martingale property, we obtain

$$\mathbb{E}\Big[\log(\|\boldsymbol{x}_{\sigma_n\wedge\zeta_\epsilon\wedge T}\|)\Big] \ge \mathbb{E}\Big[\log(\|\boldsymbol{x}_0\|)\Big] - \Big(K_n + \frac{\nu n^{2\theta}T^2}{2}\Big)T.$$

Alternatively, the upper bound of the above expectation value can be estimated as

$$\mathbb{E}\Big[\log(\|\boldsymbol{x}_{\sigma_n\wedge\zeta_\epsilon\wedge T}\|)\Big] \le \mathbb{P}(\zeta_\epsilon < \sigma_n \wedge T)\cdot\log\epsilon + \Big[1 - \mathbb{P}(\zeta_\epsilon < \sigma_n \wedge T)\Big]\cdot\log n,$$

leading to

$$\mathbb{E}\Big[\log(\|\boldsymbol{x}_0\|)\Big] - \left(K_n + \frac{\nu n^{2\theta} T^2}{2}\right) T \le \mathbb{P}(\zeta_\epsilon < \sigma_n \wedge T) \cdot \log \epsilon + \Big[1 - \mathbb{P}(\zeta_\epsilon < \sigma_n \wedge T)\Big] \cdot \log n.$$

Taking the limit $\epsilon \to 0+$ in the above inequality results in $\mathbb{P}(\zeta_0 < \sigma_n \wedge T) = 0$. Since n and T can be sufficiently large, we have $\mathbb{P}(\zeta_0 < \sigma_\infty) = 0$. This completes the proof of the first step.

Second, we are to prove that the controlled trajectory of system (2.1) does not diverge in a finite time duration. Applying Itô's formula to $\log(1+\|\boldsymbol{x}_t\|^\alpha)$ on the time interval $[0, \sigma_n \wedge t]$ yields

$$\begin{aligned}
\log(1+\|\boldsymbol{x}_{\sigma_n\wedge t}\|^\alpha) = \log(1+\|\boldsymbol{x}_0\|^\alpha) &+ \int_0^{\sigma_n\wedge t} \frac{\alpha\|\boldsymbol{x}_s\|^{\alpha-2}\langle \boldsymbol{x}_s, \boldsymbol{f}(\boldsymbol{x}_s)\rangle}{1+\|\boldsymbol{x}_s\|^\alpha}\mathrm{d}s \\
&+ \int_0^{\sigma_n\wedge t} \frac{k_s^2\|\boldsymbol{x}_s\|^{\alpha-4}}{2(1+\|\boldsymbol{x}_s\|^\alpha)}\Bigg\{\frac{\alpha^2}{1+\|\boldsymbol{x}_s\|^\alpha}\sum_{l=1}^m \Big(\boldsymbol{x}_s^\top \boldsymbol{A}_l \boldsymbol{x}_s\Big)^2 \\
&- \alpha\Big[2\sum_{l=1}^m (\boldsymbol{x}_s^\top \boldsymbol{A}_l \boldsymbol{x}_s)^2 - \sum_{l=1}^m \|\boldsymbol{x}_s\|^2 \|\boldsymbol{A}_l \boldsymbol{x}_s\|^2\Big]\Bigg\}\mathrm{d}s \\
&+ \sum_{l=1}^m \int_0^{\sigma_n\wedge t} \frac{\alpha k_s \|\boldsymbol{x}_s\|^{\alpha-2}\langle \boldsymbol{x}_s, \boldsymbol{A}_l \boldsymbol{x}_s\rangle}{1+\|\boldsymbol{x}_s\|^\alpha}\mathrm{d}B_l(s),
\end{aligned} \tag{4.4}$$

where α is a positive number to be specified. Using Condition 2.2 centered at zero, we can estimate the first integral term on the right side of (4.4) as

$$\frac{\alpha\|\boldsymbol{x}_s\|^{\alpha-2}\langle \boldsymbol{x}_s, \boldsymbol{f}(\boldsymbol{x}_s)\rangle}{1+\|\boldsymbol{x}_s\|^\alpha} \le \frac{\alpha L\|\boldsymbol{x}_s\|^\alpha}{1+\|\boldsymbol{x}_s\|^\alpha} \le \alpha L.$$

We select a sufficiently large value of M such that $\sum_{l=1}^m \left(\boldsymbol{x}^\top \boldsymbol{A}_l \boldsymbol{x}\right)^2 \le M\|\boldsymbol{x}\|^4$. This, together with Condition 2.4, allows us to estimate the second integral term on the right side of (4.4) as

$$\begin{aligned}
&\frac{k_s^2\|\boldsymbol{x}_s\|^{\alpha-4}}{2(1+\|\boldsymbol{x}_s\|^\alpha)}\left\{\frac{\alpha^2}{1+\|\boldsymbol{x}_s\|^\alpha}\sum_{l=1}^m \Big(\boldsymbol{x}_s^\top \boldsymbol{A}_l \boldsymbol{x}_s\Big)^2 - \alpha\left[2\sum_{l=1}^m (\boldsymbol{x}_s^\top \boldsymbol{A}_l \boldsymbol{x}_s)^2 - \sum_{l=1}^m \|\boldsymbol{x}_s\|^2 \|\boldsymbol{A}_l \boldsymbol{x}_s\|^2\right]\right\} \\
&\qquad \le \frac{k_s^2\|\boldsymbol{x}_s\|^{\alpha-4}}{2(1+\|\boldsymbol{x}_s\|^\alpha)}\left[\alpha^2 M\|\boldsymbol{x}_s\|^4 - 2\alpha\gamma\|\boldsymbol{x}_s\|^4\right],
\end{aligned}$$

where α is chosen to be $\alpha = \gamma/M$ with $\alpha^2 M - 2\alpha\gamma < 0$. Taking the expectation values on both sides of (4.4) and using the above estimates, we obtain

$$\mathbb{E}\Big[\log(1+\|\boldsymbol{x}_{\sigma_n\wedge T}\|^\alpha)\Big] \le \mathbb{E}\Big[\log(1+\|\boldsymbol{x}_0\|^\alpha)\Big] + \alpha L T.$$

In terms of the lower bound, the expectation value can be estimated as

$$\mathbb{E}\Big[\log(1+\|\boldsymbol{x}_{\sigma_n\wedge T}\|^\alpha)\Big] \ge \mathbb{P}(\sigma_n < T)\log(1+N^\alpha).$$

We thus have

$$\mathbb{P}(\sigma_n < T)\log(1+n^\alpha) \le \mathbb{E}\Big[\log(1+\|\boldsymbol{x}_0\|^\alpha)\Big] + \alpha L T.$$

Letting $n \to +\infty$ in the last inequality leads to $\mathbb{P}(\sigma_\infty < T) = 0$ which, after further letting $T \to +\infty$, becomes $\mathbb{P}(\sigma_\infty < +\infty) = 0$. This completes the proof of the second step.

We are now in a position to prove the following limits in the sense of almost surely:

$$\lim_{t\to+\infty} \boldsymbol{x}_t = \mathbf{0} \quad \text{and} \quad \lim_{t\to+\infty} k_t < +\infty.$$

In our proof, we use a lemma on the convergence of the semimartingale process.[1]. We decompose $\|\boldsymbol{x}_t\|^\eta$ in the same manner as Z_t in the convergence lemma of the semimartingale. To this end, an application of Itô's formula to $\|\boldsymbol{x}_t\|^\eta$ gives

$$\begin{aligned}\|\boldsymbol{x}_t\|^\eta = \|\boldsymbol{x}_0\|^\eta + \int_0^t \frac{\eta}{2}\|\boldsymbol{x}_s\|^{\eta-4}\Bigg\{ & 2\|\boldsymbol{x}_s\|^2\langle \boldsymbol{x}, \boldsymbol{f}(\boldsymbol{x})\rangle \\ & + k_s^2\left[(\eta-2)\sum_{l=1}^m \left(\boldsymbol{x}_s^\top \boldsymbol{A}_l \boldsymbol{x}_s\right)^2 + \sum_{l=1}^m \|\boldsymbol{x}_s\|^2\|\boldsymbol{A}_l\boldsymbol{x}_s\|^2\right]\Bigg\}\mathrm{d}s \\ & + \sum_{l=1}^m \int_0^t \eta k_s \|\boldsymbol{x}_s\|^{\eta-2}\left(\boldsymbol{x}_s^\top \boldsymbol{A}_l \boldsymbol{x}_s\right)\mathrm{d}B_l(t),\end{aligned} \tag{4.5}$$

where we have used Condition 2.4 to get

$$(\eta-2)\sum_{l=1}^m \left(\boldsymbol{x}^\top \boldsymbol{A}_l \boldsymbol{x}\right)^2 + \sum_{l=1}^m \|\boldsymbol{x}\|^2\|\boldsymbol{A}_l\boldsymbol{x}\|^2 \le \eta\sum_{l=1}^m \left(\boldsymbol{x}^\top \boldsymbol{A}_l \boldsymbol{x}\right)^2 - 2\gamma\|\boldsymbol{x}\|^4$$

with η being a sufficiently small and positive number with

$$\eta\sum_{l=1}^m \left(\boldsymbol{x}^\top \boldsymbol{A}_l \boldsymbol{x}\right)^2 - 2\gamma\|\boldsymbol{x}\|^4 \le -\gamma\|\boldsymbol{x}\|^4.$$

Equation (4.5) can then be rewritten as $Z_t = \xi + A_t^1 - A_t^2 + M_t$ with

$$\begin{aligned} & Z_t = \|\boldsymbol{x}_t\|^\eta, \quad \xi = \|\boldsymbol{x}_0\|^\eta, \quad A_t^1 = \int_0^t v_s \mathbf{1}_{v_s\ge 0}\mathrm{d}s, \\ & A_t^2 = -\int_0^t v_s \mathbf{1}_{v_s<0}\mathrm{d}s, \quad M_t = \sum_{l=1}^m \int_0^t \eta k_s\|\boldsymbol{x}_s\|^{\eta-2}\left(\boldsymbol{x}_s^\top \boldsymbol{A}_l \boldsymbol{x}_s\right)\mathrm{d}B_l(s), \end{aligned}$$

[1] **Lemma** (convergence of semimartingale) [38] Let A^1 and A^2 be nondecreasing processes with $A_0^1 = A_0^2 = 0$. Let Z be a nonnegative semimartingale with an initial state $\mathbb{E}Z_0 < +\infty$ and

$$Z_t = Z_0 + A_t^1 - A_t^2 + M_t, \quad t \ge 0,$$

where M is a local martingale with $M_0 = 0$. If A^1 is a continuous process, then we have almost surely

$$\begin{aligned}\left\{\omega : A^1(+\infty) < +\infty\right\} \subseteq \left\{\omega : \lim_{t\to+\infty} Z_t \text{ exists finitely}\right\} \cap \left\{\omega : A^2(+\infty) < +\infty\right\} \\ \cap\left\{\omega : \lim_{t\to+\infty} M_t \text{ exists finitely}\right\}.\end{aligned}$$

where $\mathbf{1}_{\mathcal{S}}$ is the standard indicator function with respect to the given set $\mathcal{S}$ and

$$v_t = \frac{\eta}{2}\|\boldsymbol{x}_s\|^{\eta-4}\left\{2\|\boldsymbol{x}_s\|^2\langle \boldsymbol{x}, \boldsymbol{f}(\boldsymbol{x})\rangle + k_s^2\left[(\eta-2)\sum_{l=1}^{m}\left(\boldsymbol{x}_s^\top \boldsymbol{A}_l \boldsymbol{x}_s\right)^2 + \sum_{l=1}^{m}\|\boldsymbol{x}_s\|^2\|\boldsymbol{A}_l\boldsymbol{x}_s\|^2\right]\right\}.$$

From the estimation

$$2\|\boldsymbol{x}_s\|^2\langle \boldsymbol{x}, \boldsymbol{f}(\boldsymbol{x})\rangle + k_s^2\left[(\eta-2)\sum_{l=1}^{m}\left(\boldsymbol{x}_s^\top \boldsymbol{A}_l \boldsymbol{x}_s\right)^2 + \sum_{l=1}^{m}\|\boldsymbol{x}_s\|^2\|\boldsymbol{A}_l\boldsymbol{x}_s\|^2\right] \leq 2L\|\boldsymbol{x}_s\|^4 - k_s^2\gamma\|\boldsymbol{x}_s\|^4,$$

we have that $v_t \leq 0$ for $k_s \geq \sqrt{2L/\gamma}$. Denote the stopping time as

$$\kappa \triangleq \inf\left\{t \geqslant 0 : k_t \geq \sqrt{2L/\gamma}\right\}.$$

Due to the fact that k_t is an increasing function of t, we have $v_t < 0$ for $t > \kappa$, which further implies $A_\infty^1 < +\infty$ almost certainly in the set $\{\kappa < +\infty\}$. According to the lemma of the convergence of a semimartingale, we conclude that almost surely $\lim_{t\to+\infty}\|\boldsymbol{x}_t\|^\eta$ exists and is finite in the set $\{\kappa < +\infty\}$.

Moreover, the limit $\lim_{t\to+\infty} M_t$ exists and is finite almost certainly in the set $\{\kappa < +\infty\}$, further indicating that the limit of the quadratic variation of M_t, $\lim_{t\to+\infty}[M_t, M_t]$, almost surely exists and is finite. Thus, for almost every sample in the set $\{\kappa < +\infty\}$, we have

$$\int_0^{+\infty} \eta^2 k_s^2 \|\boldsymbol{x}_s\|^{2\eta-4}\sum_{l=1}^{m}\left(\boldsymbol{x}_s^\top \boldsymbol{A}_l \boldsymbol{x}_s\right)^2 \mathrm{d}s < +\infty.$$

This, together with Condition 2.4 and the increasing property of k_t, results in $\int_0^{+\infty}\|\boldsymbol{x}_s\|^{2\eta}\mathrm{d}s < +\infty$ almost surely in the set $\{\kappa < +\infty\}$. Notice the fact that the existence and the finiteness of $\lim_{t\to+\infty}\|\boldsymbol{x}_t\|^\eta$ have been validated above. We thus have $\lim_{t\to+\infty}\|\boldsymbol{x}_t\| = 0$ almost surely in the set $\{\kappa < +\infty\}$. In addition, noting the boundedness of $\|\boldsymbol{x}_t\|$ on the entire interval $[0, +\infty)$, we get

$$k_\infty = \int_0^{+\infty}\|\boldsymbol{x}_s\|^\theta \mathrm{d}s \leq \sup_{0\leq t<+\infty}\|\boldsymbol{x}_t\|^{\theta-2\eta}\int_0^{+\infty}\|\boldsymbol{x}_s\|^{2\eta}\mathrm{d}s < +\infty$$

almost surely in the set $\{\kappa < +\infty\}$.

To impose a restriction inside the set $\{\kappa = +\infty\}$, we define the functional

$$V_t = \|\boldsymbol{x}_{t\wedge\kappa}\|^\theta - \theta L k_{t\wedge\kappa} - \frac{1}{6}\theta M k_{t\wedge\kappa}^3,$$

where M is a positive number to be specified. By Itô's formula, V_t can be decomposed as

$V_t = \|\boldsymbol{x}_0\|^\theta + C_t^1 - C_t^2 + N_t$, where

$$
\begin{aligned}
C_t^1 &\equiv 0,\\
C_t^2 &= -\int_0^{t\wedge\kappa} \frac{\theta}{2}\|\boldsymbol{x}_s\|^{\theta-4}\Big\{ \left[2\|\boldsymbol{x}_s\|^2\langle \boldsymbol{x}_s, \boldsymbol{f}(\boldsymbol{x}_s)\rangle - L\|\boldsymbol{x}_s\|^4\right]\\
&\quad + k_s^2\left[(\theta-2)\sum_{l=1}^m \left(\boldsymbol{x}_s^\top \boldsymbol{A}_l \boldsymbol{x}_s\right)^2 + \sum_{l=1}^m \|\boldsymbol{x}_s\|^2\|\boldsymbol{A}_l\boldsymbol{x}_s\|^2 - M\|\boldsymbol{x}_s\|^4\right]\Big\}\mathrm{d}s,\\
N_t &= \sum_{l=1}^m \int_0^{t\wedge\kappa} \theta k_s \|\boldsymbol{x}_s\|^{\theta-2}\left(\boldsymbol{x}_s^\top \boldsymbol{A}_l \boldsymbol{x}_s\right)\mathrm{d}B_l(s).
\end{aligned}
$$

It can be seen that V_t has a uniform lower bound. From a different angle, we have that C_t^2 is an adaptive and nondecreasing process when M is chosen to be a sufficiently large number. Applying the convergence lemma of a semimartingale again gives that $\lim_{t\to+\infty} V_t$ exists and is finite in the sense of almost surely. In the set $\{\kappa = +\infty\}$, due to the boundedness of k_t, we have $\lim_{t\to+\infty} k_t$ exists and is finite, further indicating that $\lim_{t\to+\infty}\|\boldsymbol{x}_t\|^\theta$ exists and is finite in the set $\{\kappa = +\infty\}$. Furthermore, the fact that $\lim_{t\to+\infty} k_t = \int_0^{+\infty}\|\boldsymbol{x}_s\|^\theta \mathrm{d}s < \infty$ gives rise to $\lim_{t\to+\infty}\|\boldsymbol{x}_t\| = 0$ in the set $\{\kappa = +\infty\}$. This completes the proof of the theorem. ∎

Remark 4.1. If Condition 2.2 is not assumed, we can replace $\boldsymbol{x}_t$ by $\boldsymbol{x}_{t\wedge\sigma_{n+1}}$ in the above proof. This replacement, together with the inequality (4.2), allows us to validate

$$\lim_{t\to+\infty}\|\boldsymbol{x}_t\| = 0 \quad \text{and} \quad \lim_{t\to\infty} k_t < +\infty$$

almost everywhere in the set

$$\mathcal{E}_n = \Big\{\omega\in\Omega : \|\boldsymbol{x}_t(\omega)\| \le n \text{ for } t\in[0,+\infty)\Big\}.$$

As a result, the above two limits also exist almost surely in the set $\mathcal{E} = \bigcup_{n=1}^\infty \mathcal{E}_n$, leading to the next corollary.

Corollary 4.2. *Assume that both Condition 2.1 and Condition 2.4 hold. For almost every sample trajectory $\boldsymbol{x}_t$ of the controlled system (2.1), it either diverges or converges to zero. Particularly, when it converges to zero, $\lim_{t\to+\infty} k_t < +\infty$ holds almost surely.*

Proof of Theorem 3.4. To prove the theorem, we need to obtain an estimate of the probability $\mathbb{P}(\sigma_n < +\infty)$ by using the theory of martingale and Condition 2.5. We define a functional $W_t = \|\boldsymbol{x}_t\|^\theta - K_n k_t + \frac{1}{6}\theta h k_t^3$. Using Itô's formula to W_t gives

$$
\begin{aligned}
W_{t\wedge\sigma_n} &= \|\boldsymbol{x}_0\|^\theta + \int_0^{t\wedge\sigma_n} \frac{\theta}{2}\|\boldsymbol{x}_s\|^{\theta-4}\Big\{ \left(2\|\boldsymbol{x}_s\|^2\langle \boldsymbol{x}_s, \boldsymbol{f}(\boldsymbol{x}_s)\rangle - K_n\|\boldsymbol{x}_s\|^4\right)\\
&\quad + k_s^2\left[(\theta-2)\sum_{l=1}^m \left(\boldsymbol{x}_s^\top \boldsymbol{A}_l \boldsymbol{x}_s\right)^2 + \sum_{l=1}^m \|\boldsymbol{x}_s\|^2\|\boldsymbol{A}_l\boldsymbol{x}_s\|^2 + h\|\boldsymbol{x}_s\|^4\right]\Big\}\mathrm{d}s\\
&\quad + \sum_{l=1}^m \int_0^{t\wedge\sigma_n} \theta k_s \|\boldsymbol{x}_s\|^{\theta-2}\left(\boldsymbol{x}_s^\top \boldsymbol{A}_l \boldsymbol{x}_s\right)\mathrm{d}B_l(s).
\end{aligned}
\tag{4.6}
$$

Taking the expectation values of both sides of (4.6), we obtain

$$\mathbb{E}\left[\|\boldsymbol{x}_{T\wedge\sigma_n}\|^\theta - K_n k_{T\wedge\sigma_n} + \frac{1}{6}\theta h k_{T\wedge\sigma_n}^3\right] \leq \mathbb{E}\|\boldsymbol{x}_0\|^\theta,$$

which, after appropriate steps of analysis and estimation, gives

$$\mathbb{E}\|\boldsymbol{x}_{T\wedge\sigma_n}\|^\theta \leq \mathbb{E}\|\boldsymbol{x}_0\|^\theta + \mathbb{E}\left[K_n k_{T\wedge\sigma_n} - \frac{1}{6}\theta h k_{T\wedge\sigma_n}^3\right] \leq \mathbb{E}\|\boldsymbol{x}_0\|^\theta + \sqrt{8K_n^3/9\theta h}.$$

This, with $\mathbb{E}\|\boldsymbol{x}_{T\wedge\sigma_n}\|^\theta \geq n^\theta \mathbb{P}(\sigma_n \leq T)$, implies

$$n^\theta \mathbb{P}(\sigma_n \leq T) \leq \mathbb{E}\|\boldsymbol{x}_0\|^\theta + \sqrt{8K_n^3/9\theta h}.$$

Letting $T \to +\infty$ leads to the expected estimate of the probability as

$$\mathbb{P}(\sigma_n < +\infty) \leq \frac{\mathbb{E}\|\boldsymbol{x}_0\|^\theta + \sqrt{8K_n^3/9\theta h}}{n^\theta}.$$

Using the condition $\lim_{n\to+\infty} K_n^{3/2}/n^\theta = 0$ as assumed in (3.1), we have

$$\mathbb{P}(\mathcal{E}^c) = \mathbb{P}\left(\bigcap_{n=1}^{+\infty} \mathcal{E}_n^c\right) = \lim_{n\to+\infty} \mathbb{P}(\sigma_n < +\infty) = 0.$$

Consequently, in light of Corollary 4.2, we have completed the proof. The significance is that stochastically adaptive feedback controller is effective for stabilizing systems that are only locally one-sided Lipschitzian in the sense of probability one. ∎

Proof of Theorem 3.7. Denote $\boldsymbol{z}_t \triangleq \boldsymbol{y}_t - \boldsymbol{x}_t$. The dynamical evolution of the error between the driving (3.3) and the response (3.4) systems is governed by

$$\mathrm{d}\boldsymbol{z}_t = \Big[\boldsymbol{f}(\boldsymbol{y}_t) - \boldsymbol{f}(\boldsymbol{x}_t)\Big]\mathrm{d}t + \sum_{l=1}^{m}(k_t \boldsymbol{A}_l)\boldsymbol{z}_t \mathrm{d}B_l(t).$$

The inequality in Condition 2.2 can be written as

$$\big\langle \boldsymbol{z}_t, \boldsymbol{f}(\boldsymbol{y}_t) - \boldsymbol{f}(\boldsymbol{x}_t)\big\rangle \leq L\|\boldsymbol{z}_t\|^2,$$

which is analogous to Condition 2.2 centered at zero assumed for the control system (2.1). Employing a similar line of arguments for proving Theorem 3.2, we can prove, in the sense of almost surely, the following two limits: $\lim_{t\to+\infty}\|\boldsymbol{z}_t\| = 0$ and $\lim_{t\to+\infty} k_t < +\infty$. ∎

5. Examples. We provide a number of concrete examples to demonstrate the use of the mathematical theorems developed in the two preceding sections.

Example 5.1. We consider two cases to assess the circumstances under which the matrices $\boldsymbol{A}_l$ with Brownian processes of different dimensions satisfy Condition 2.4, which will be employed in the examples.

For the first case, we consider a one-dimensional Brownian process for a three-dimensional controlled system (2.1). To be specific, we choose the matrix $\boldsymbol{A}_1$ to be diagonal: $\boldsymbol{A}_1 = \mathrm{diag}\{a_1, a_2, a_3\}$. We apply the method of Lagrange multipliers [62] to analytically determine the feasibility region of parameters a_i that fulfills Condition 2.4. Since inequality (2.2) is homogeneous with respect to the argument $\boldsymbol{x}$, it suffices to find the region of parameters a_i such that, for any $\boldsymbol{x}$ with $\|\boldsymbol{x}\| = 1$,

$$\left(\boldsymbol{x}^\top \boldsymbol{A}_1 \boldsymbol{x}\right)^2 - \frac{1}{2}\|\boldsymbol{A}_1 \boldsymbol{x}\|^2 \geq \gamma > 0. \tag{5.1}$$

We set the Lagrange function as $\mathscr{L}(\boldsymbol{x}, \lambda) = F(\boldsymbol{x}) - \lambda(\|\boldsymbol{x}\|^2 - 1)$ with λ being the Lagrange multiplier, $\boldsymbol{x} = (x_1, x_2, x_3)^\top$, and

$$F(\boldsymbol{x}) = \left(\boldsymbol{x}^\top \boldsymbol{A}_1 \boldsymbol{x}\right)^2 - \frac{1}{2}\|\boldsymbol{A}_1 \boldsymbol{x}\|^2 = \left(a_1 x_1^2 + a_2 x_2^2 + a_3 x_3^2\right)^2 - \frac{1}{2}\left(a_1^2 x_1^2 + a_2^2 x_2^2 + a_3^2 x_3^2\right).$$

Accordingly, from the partial derivatives

$$\frac{\partial \mathscr{L}}{\partial x_i} = x_i\left[4a_i\left(a_1 x_1^2 + a_2 x_2^2 + a_3 x_3^2\right) - a_i^2 - 2\lambda\right] = 0, \quad i = 1, 2, 3, \tag{5.2}$$

we have that, for each i, either $x_i = 0$ or $4a_i\left(a_1 x_1^2 + a_2 x_2^2 + a_3 x_3^2\right) - a_i^2 - 2\lambda = 0$, which gives the stationary point (x_1, x_2, x_3, λ). Consider the situation where a_i $(i = 1, 2, 3)$ are mutually distinct. For any stationary point with $\|\boldsymbol{x}\| = 1$, if any two components of $\boldsymbol{x}$ equal zero, the remaining component, say, x_i, is either 1 or -1. We thus have $F(\boldsymbol{x}) = (1/2)a_i^2 > 0$. If only one component of $\boldsymbol{x}$ is zero (denoted by x_3), we have

$$4a_i\left(a_1 x_1^2 + a_2 x_2^2\right) - a_i^2 - 2\lambda = 0, \quad i = 1, 2,$$

which implies

$$a_1 x_1^2 + a_2 x_2^2 = \frac{a_1 + a_2}{4}.$$

This, together with the constraint $\|\boldsymbol{x}\| = 1$ (i.e., $x_1^2 + x_2^2 = 1$), leads to

$$x_1^2 = \frac{a_1 - 3a_2}{4a_1 - 4a_2}, \quad x_2^2 = \frac{a_2 - 3a_1}{4a_2 - 4a_1},$$

which are solvable only if $a_1 \geq 3a_2$ or $a_2 \geq 3a_1$. Thus, $F(\boldsymbol{x}) = (-a_1^2 - a_2^2 + 6a_1 a_2)/16$ approaches a positive extreme value if and only if $a_1 < (3 + 2\sqrt{2})a_2$ and $a_2 < (3 + 2\sqrt{2})a_1$. If none of the components of $\boldsymbol{x}$ is zero, we have $a_1 x_1^2 + a_2 x_2^2 + a_3 x_3^2 = \frac{1}{4}(a_i + a_j)$ for $i \neq j$, contradicting the assumption that a_i are mutually distinct.

For the case where a_i are not mutually different, a similar analysis can be carried out. Taken together, we have that the minimal value of $F(\boldsymbol{x})$ is positive if and only if $a_i < (3 + 2\sqrt{2})a_j$ for any $i, j = 1, 2, 3$ with $i \neq j$. This circumscribed region of parameters a_i contains the condition obtained for the first case. A numerically determined region is shown in Figure 1(a).

The second case is where the Brownian process is two-dimensional. We consider matrices of the following form:

$$\boldsymbol{A}_1 = \begin{bmatrix} 1 & 0 & 0 \\ a_1 & 1 & 0 \\ 0 & 0 & 1 \end{bmatrix}, \quad \boldsymbol{A}_2 = \begin{bmatrix} 1 & 0 & 0 \\ 0 & 1 & a_2 \\ 0 & 0 & 1 \end{bmatrix}$$

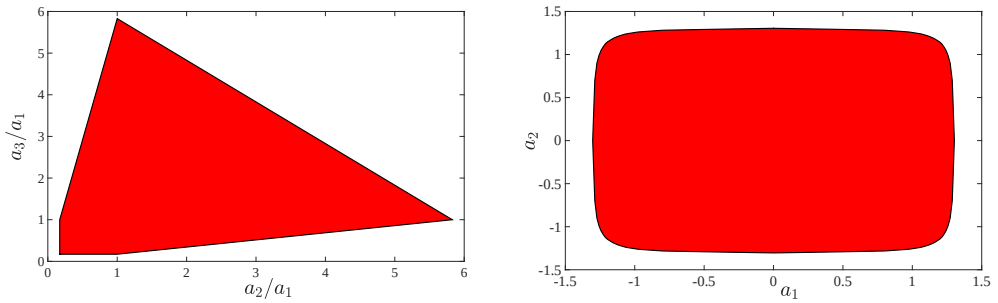

(a) (b)

Figure 1. *Feasible parameter regions satisfying Condition 2.4.* (a) *The circumscribed region obtained based on (5.1) for the case of a one-dimensional Brownian process and three parameters $a_{1,2,3}$.* (b) *The circumscribed region fulfilling (5.3) for the case of a two-dimensional Brownian process and two parameters $a_{1,2}$.*

with two parameters a_1 and a_2. Akin to the first case, it is necessary to find the parameter region satisfying the condition that, for all $\|\boldsymbol{x}\| = 1$,

$$\sum_{l=1}^{2}\left(\boldsymbol{x}^{\top}\boldsymbol{A}_l\boldsymbol{x}\right)^2 - \frac{1}{2}\sum_{l=1}^{2}\|\boldsymbol{A}_l\boldsymbol{x}\|^2 \geq \gamma > 0. \tag{5.3}$$

Numerical evaluation of this condition yields a symmetric and round rectangle region for the parameters a_1 and a_2, as shown in Figure 1(b).

Example 5.2. We implement the stochastically adaptive feedback controller (2.1) to stabilize the classic Lorenz system [39]. The controlled system can be written as

$$\begin{cases} \mathrm{d}x_1 = (\sigma x_2 - \sigma x_1)\mathrm{d}t + ka_1x_1\mathrm{d}B_t, \\ \mathrm{d}x_2 = (\rho x_1 - x_3x_1 - x_2)\mathrm{d}t + ka_2x_2\mathrm{d}B_t, \\ \mathrm{d}x_3 = (x_1x_2 - \beta x_3)\mathrm{d}t + ka_3x_3\mathrm{d}B_t, \\ \mathrm{d}k = (x_1^2 + x_2^2 + x_3^2)^{\frac{\theta}{2}}\mathrm{d}t, \end{cases} \tag{5.4}$$

for $\sigma = 10$, $\rho = 28$, $\beta = 8/3$, $a_1 = 1$, $a_2 = 2$, and $a_3 = 4$. In the absence of control, system (5.4) exhibits chaotic dynamics, as shown in Figure 2(a). Notice that

$$\begin{aligned} &\big\langle (x_1, x_2, x_3), (\sigma x_2 - \sigma x_1, \rho x_1 - x_3x_1 - x_2, x_1x_2 - \beta x_3)\big\rangle \\ &\quad = (\sigma + \rho)x_1x_2 - \sigma x_1^2 - x_2^2 - \beta x_3^2 \leq \frac{\sigma + \rho}{2}(x_1^2 + x_2^2 + x_3^2). \end{aligned}$$

Thus, the vector field of the uncontrolled system satisfies both Condition 2.1 and Condition 2.2 centered at zero. Using the constraints for the one-dimensional Brownian process in Example 5.1, the diagonal matrix $\boldsymbol{A}_1 = \mathrm{diag}\{a_1, a_2, a_3\}$ satisfies Condition 2.4. Hence, the conditions required in Theorem 3.2 are all fulfilled, guaranteeing that the controlled trajectory $\boldsymbol{x}_t$ of system (5.4) can be stabilized to its steady state solution in the physical sense of almost surely. Numerical confirmation is shown in Figures 2(b) to 2(d), where Milstein's discretization algorithm [31] with step size $\triangle t = 10^{-6}$ is used for integrating the system of stochastic differential equations. Specifically, for different values of $\theta > 0$, the stochastically adaptive

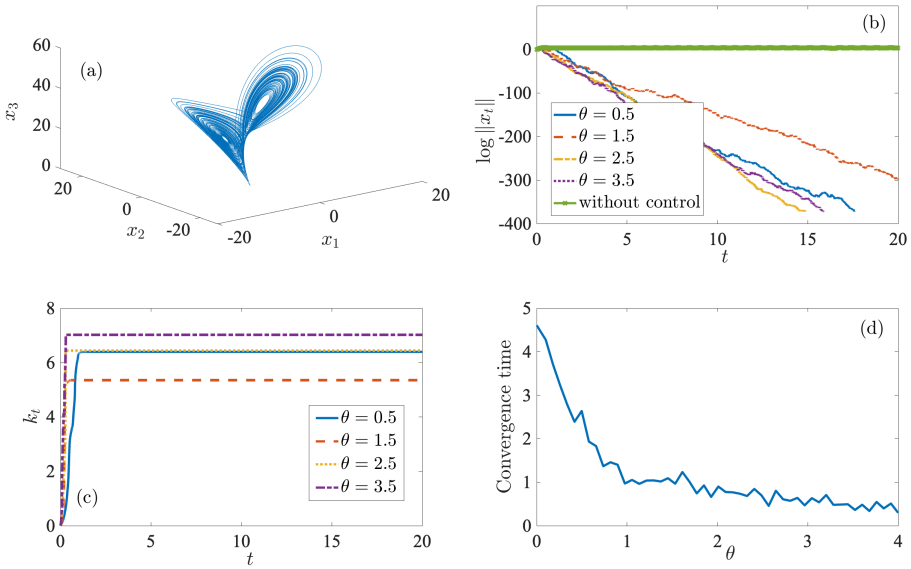

Figure 2. *Uncontrolled and controlled Lorenz system* (5.4). *The initial conditions are* $\boldsymbol{x}_0 = [1, 2, 3]^\top$. (a) *Classic chaotic dynamics of the uncontrolled Lorenz system.* (b) *For different values of* θ, *the controlled trajectory converges to the target state exponentially with different rate values.* (c) *Convergence of the gain* k_t *to different constant values.* (d) *Time required of convergence for the controlled system* (5.4) *for different values of* θ, *where the convergence time is counted as the left-side time instant of a* T*-length time interval during which the absolute value of the controlled states* $\boldsymbol{x}_t$ *is less than* 10^{-4}. *In* (d), $T = 1$ *and each value of the convergence time is obtained by averaging the times of* 1000 *random realizations of the controlled system.*

feedback controller makes the controlled system convergent exponentially (Figure 2(b)) and the corresponding coupling strength k_t converges to some constant (Figure 2(c)). In addition, as shown in Figure 2(d), the convergence time of the controlled system displays a decreasing tendency with an increase of θ, despite a few fluctuations aroused by the stochastic perturbations (see Figure 3).

Example 5.3. To assess the extent to which the locally Lipschitzian condition leads to successful stochastic stabilization, we consider a one-dimensional vector field $f(x) = |x|^d \mathrm{sgn}(x)$, where the index $d \geq 1$ characterizes the degree of nonlinearity of the vector field. From Theorem 3.4 and Corollary 3.5, the controlled system can be written as

$$\mathrm{d}x_t = f(x_t)\mathrm{d}t + k_t x_t \mathrm{d}B_t, \quad \mathrm{d}k_t = |x|^\theta \mathrm{d}t. \tag{5.5}$$

Using the condition in (3.1) or (3.2), we get

$$1 \leq d < 1 + \frac{2\theta}{3} \text{ for } \theta < 1, \tag{5.6}$$

rendering the vector field a locally Lipschitzian function. However, there is an analytical ceiling on the degree of nonlinearity of such a function for successful realization of stochastic stabilization of controlled system (5.5). As shown in Figure 4 numerically, for each value of θ, there is a threshold d_c above which the stochastic stabilization always fails exactly and below

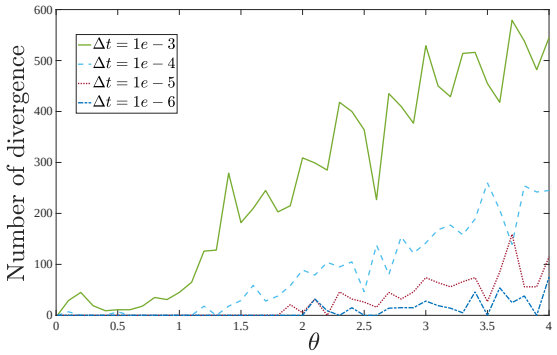

Figure 3. *The number of divergent cases over* 1000 *random realizations for the stochastically controlled system* (5.4) *with different values of power* θ *and integration step size* $\triangle t$*. For a fixed value of* θ*, a smaller value of* $\triangle t$ *leads to less divergence. For* $\theta \in (2,4)$*, there is a nonzero probability that the feedback control scheme fails numerically (even with step size as small as* $\triangle t = 10^{-6}$*).*

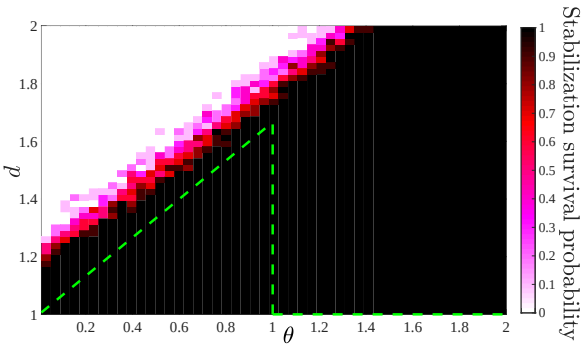

Figure 4. *Dependence of probability of successful stabilization on power* θ *and nonlinear index* d *for controlled system* (5.5)*. The initial values are* $x_0 = 10$ *and* $k_0 = 0$*. The success probability is estimated as the frequency of the stochastic stabilization from* 100 *numerical realizations of the controlled system* (5.5)*. The dashed (green) curves indicate the boundary obtained from the analytical constraint* (5.6) *for* θ *and* d*.*

which it succeeds with a large probability. The numerical threshold d_c tends to be larger than the analytical constraint in (5.6), indicating that our criterion is only a sufficient condition, leaving room for further improvement.

Example 5.4. We consider stochastic synchronization between two Hindmarsh–Rose neurons with spiking dynamics [72], which are coupled unidirectionally according to (3.4):

$$
(5.7)\quad \begin{cases}
\mathrm{d}x_1 = (x_2 - x_1^3 + 3x_1^2 - x_3 + 3)\mathrm{d}t, \\
\mathrm{d}x_2 = (1 - 5x_1^2 - x_2)\mathrm{d}t, \\
\mathrm{d}x_3 = 0.01(4x_1 + 6.4 - x_3)\mathrm{d}t, \\
\mathrm{d}y_1 = (y_2 - y_1^3 + 3y_1^2 - y_3 + 3)\mathrm{d}t + k(y_1 - x_1)\left[\mathrm{d}B_1(t) + \mathrm{d}B_2(t)\right], \\
\mathrm{d}y_2 = (1 - 5y_1^2 - y_2)\mathrm{d}t \\
\qquad\quad + k(y_2 - x_2)\left[\mathrm{d}B_1(t) + \mathrm{d}B_2(t)\right] + 0.5k(y_1 - x_1)\mathrm{d}B_1(t) + k(y_3 - x_3)\mathrm{d}B_2(t), \\
\mathrm{d}y_3 = 0.01(4y_1 + 6.4 - y_3)\mathrm{d}t + k(y_3 - x_3)\left[\mathrm{d}B_1(t) + \mathrm{d}B_2(t)\right], \\
\mathrm{d}k = \left[(y_1 - x_1)^2 + (y_2 - x_2)^2 + (y_3 - x_3)^2\right]^{\frac{\theta}{2}}\mathrm{d}t,
\end{cases}
$$

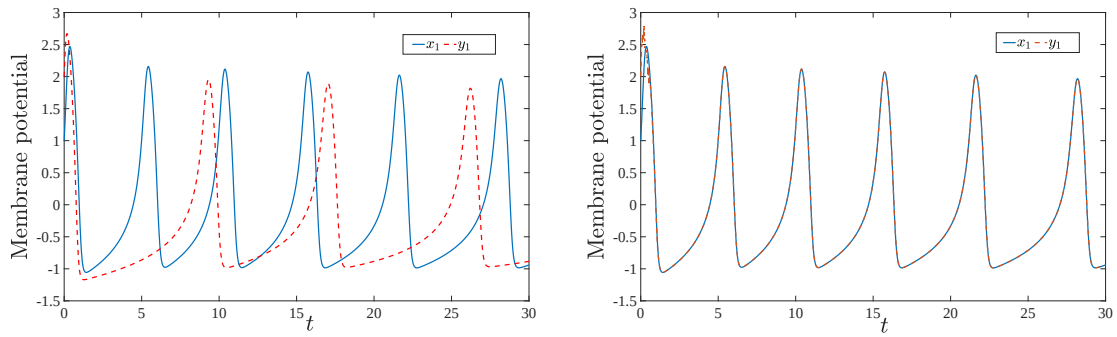

Figure 5. *Dynamics of membrane potential variables of a system of two coupled Hindmarsh–Rose neurons.* (a) *Unsynchronized dynamics without control and* (b) *synchronized dynamics with the stochastically adaptive coupling scheme. The initial and power values are, respectively,* $\boldsymbol{x}_0 = [1,1,1]^\top$, $\boldsymbol{y}_0 = [2,2,2]^\top$, *and* $\theta = 1$.

where $\boldsymbol{B}(t) = [B_1(t), B_2(t)]^\top$ is a two-dimensional Brownian process with the constant matrices $\boldsymbol{A}_{1,2}$ satisfying the requirement (5.3) of the second case in Example 5.1 and fulfilling Condition 2.4 as well. Numerical results in Figure 5 confirm the working and power of the stochastically adaptive coupling scheme (5.7).

It is worthwhile to mention that the uncontrolled vector field $\boldsymbol{f}([x_1,x_2,x_3]^\top) \triangleq [x_2 - x_1^3 + 3x_1^2 - x_3 + 3, 1 - 5x_1^2 - x_2, 0.01(4x_1 + 6.4 - x_3)]^\top$ does not satisfy the globally one-sided condition in the whole space. To see this, we compute

$$\begin{aligned}
&\boldsymbol{f}([y_1,y_2,y_3]^\top) - \boldsymbol{f}([x_1,x_2,x_3]^\top)\\
&= [(y_2 - x_2) - (y_1^3 - x_1^3) + 3(y_1^2 - x_1^2) - (y_3 - x_3),\\
&\qquad -5(y_1^2 - x_1^2) - (y_2 - x_2), 0.04(y_1 - x_1) - 0.01(y_3 - x_3)]^\top,
\end{aligned}$$

which yields estimations as follows:

$$\begin{aligned}
&\big\langle (y_1,y_2,y_3) - (x_1,x_2,x_3), \boldsymbol{f}([y_1,y_2,y_3]^\top) - \boldsymbol{f}([x_1,x_2,x_3]^\top)\big\rangle\\
&\le 2\|\boldsymbol{y} - \boldsymbol{x}\|^2 + 3(y_1^2 - x_1^2)(y_1 - x_1) - 5(y_1^2 - x_1^2)(y_2 - x_2) \le 2\|\boldsymbol{y} - \boldsymbol{x}\|^2 + 8|y_1 + x_1|\|\boldsymbol{y} - \boldsymbol{x}\|^2.
\end{aligned}$$

However, numerically, we have the boundedness as $|x_1| \le 3$ and $|y_1| \le 3$ when the trajectory is close to the synchronization manifold of system (5.7) (see Figure 5). This boundedness, together with the estimations obtained above, indicates that $\boldsymbol{f}$ satisfies the one-sided condition in the vicinity of the synchronization manifold.

Additionally, we investigate how θ, the power, and $\boldsymbol{y}_0$, the initial state of the response system, affect the synchronization time of the controlled system. As generally shown in Figure 6, the larger the value of θ, the shorter the time duration for achieving the synchronization stochastically. More interestingly, the farther the initial states between the two systems, the shorter the time duration for achieving the synchronization.

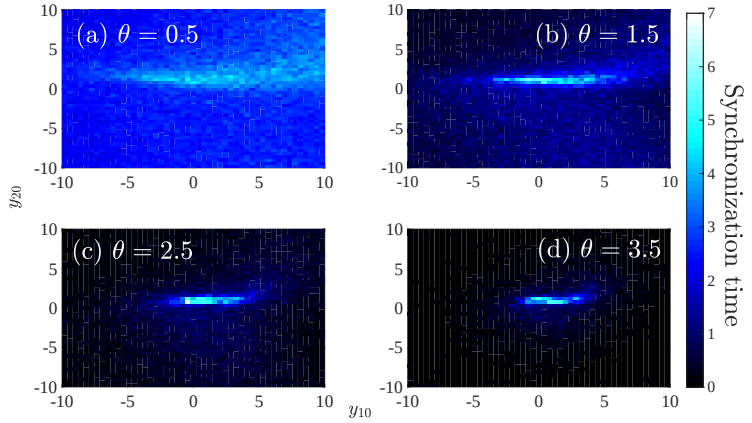

Figure 6. *For different values of θ, depicted are the synchronization times for the two stochastically coupled Hindmarsh–Rose neurons (5.7) with the initial states $\boldsymbol{x}_0 = [1,1,1]^\top$ and $\boldsymbol{y}_0 = [y_{10}, y_{20}, 0]^\top$. Here, the elements y_{10} and y_{20} are set as the alterable values. The synchronization time is counted as the left-side time instant of a 1-length time interval during which the absolute value of $\|\boldsymbol{y}_t - \boldsymbol{x}_t\|$ is less than 10^{-4}. The color of each point represents the synchronization time for any given y_{10} and y_{20}. This synchronization time is computed by averaging the corresponding times of 1000 random realizations of the controlled system.*

Example 5.5. We test stochastic synchronization in a complex networked system with a common driving signal:

$$
\begin{cases}
\mathrm{d}x_1^i = \left[\sigma x_2^i - \sigma x_1^i + \sum\limits_{j\neq i}^{N} c_{ij}(x_1^j - x_1^i)\right]\mathrm{d}t + k_t(x_1^i - u_1)\mathrm{d}B_t, \\
\mathrm{d}x_2^i = \left[\rho x_1^i - x_3^i x_1^i - x_2^i + \sum\limits_{j\neq i}^{N} c_{ij}(x_2^j - x_2^i)\right]\mathrm{d}t + k_t(x_2^i - u_2)\mathrm{d}B_t, \\
\mathrm{d}x_3^i = \left[x_1^i x_2^i - \beta x_3^i + \sum\limits_{j\neq i}^{N} c_{ij}(x_3^j - x_3^i)\right]\mathrm{d}t + k_t(x_3^i - u_3)\mathrm{d}B_t,
\end{cases}
\tag{5.8}
$$

where $\boldsymbol{u}(t) = [u_1(t), u_2(t), u_3(t)]^\top$ represents the common signal from a driving system—the Lorenz system with the parameters as specified in Example 5.2. For simplicity, we consider the following scheme for adaptively adjusting the coupling gain k_t:

$$
\mathrm{d}k = \left[(x_1^1 - u_1)^2 + (x_2^1 - u_2)^2 + (x_3^1 - u_3)^2\right]^{\frac{\theta}{2}}\mathrm{d}t,
$$

where only the difference between the common driving signal and the dynamics of the first node in the complex network is taken into account. Without the common signal, the dynamics of the network are unsynchronized when each interaction term c_{ij} is independently selected from a uniform distribution (e.g., $\mathscr{U}(0, 0.02)$), as shown in Figure 7(a). When the stochastically adaptive feedback scheme is used for the common input, the network dynamics are synchronized, as shown in Figure 7(b). This example further demonstrates the working of the stochastically adaptive schemes in achieving random synchronization.

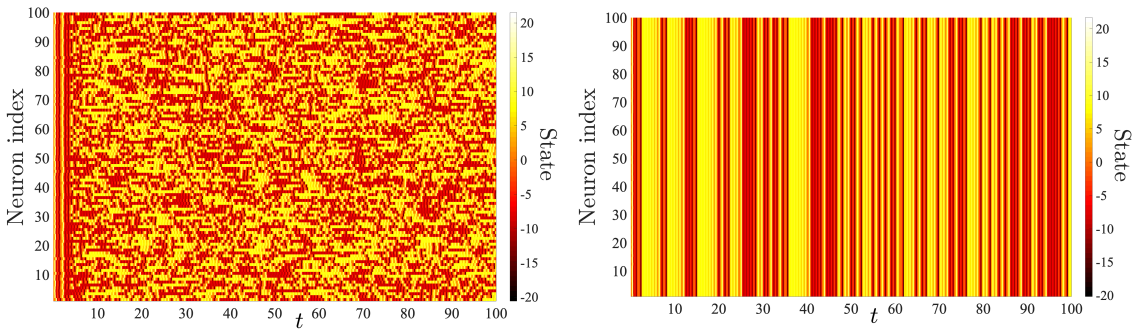

Figure 7. *Dynamics of the first state variable of each node in complex network* (5.8). (a) *Unsynchronized dynamics without any common driving signal and* (b) *synchronized dynamics generated by the stochastically adaptive coupling scheme with a common driving signal. The value of the power is* $\theta = 0.2$.

6. Applications to parameter identification. To further illustrate the effectiveness of the developed framework of stochastic synchronization, we demonstrate its application to a challenging problem in nonlinear dynamics: parameter identification. Consider a system with a group of unknown parameters, described by

$$\mathrm{d}\boldsymbol{x} = \boldsymbol{F}(\boldsymbol{x}, \boldsymbol{\mu})\mathrm{d}t, \tag{6.1}$$

where the vector field $\boldsymbol{F}$ satisfies the globally one-sided Lipschitzian Condition 2.2 with Lipschitzian constant $\boldsymbol{L}$. Elementwise, $\boldsymbol{F}$ is written as

$$F_i(\boldsymbol{x}, \boldsymbol{\mu}) = c_i(\boldsymbol{x}) + \sum_{j=1}^{m} \mu_{ij} f_{ij}(\boldsymbol{x}), \quad i = 1, 2, \ldots, p,$$

where the parameters $\boldsymbol{\mu} = \{\mu_{ij}\}$ are unknown, and the solution of system (6.1) exists and is bounded on the entire interval $[0, +\infty)$. The stochastically adaptive coupling scheme for parameter identifications is designed as

$$\mathrm{d}\boldsymbol{y} = \boldsymbol{F}(\boldsymbol{y}, \boldsymbol{v})\mathrm{d}t + k \cdot g(\|\boldsymbol{y} - \boldsymbol{x}\|) \cdot (\boldsymbol{y} - \boldsymbol{x})\mathrm{d}B_t, \tag{6.2}$$

where the estimators $\boldsymbol{v} = \{v_{ij}\}$ and the coupling gain k are, respectively, adjusted according to the following rules:

$$\mathrm{d}v_{ij} = -f_{ij}(\boldsymbol{y})V'(\|\boldsymbol{y} - \boldsymbol{x}\|)(y_i - x_i)/\|\boldsymbol{y} - \boldsymbol{x}\|\mathrm{d}t, \quad i = 1, \ldots, p, \quad j = 1, \ldots, m,$$

and

$$\mathrm{d}k = h(\|\boldsymbol{y} - \boldsymbol{x}\|)\mathrm{d}t.$$

The functions V, g, and h satisfy the following specific conditions.

Condition 6.1. The function V, defined on $[0, +\infty) \to [0, +\infty)$, is twice differentiable and satisfies $V(0) = 0$, $\lim_{x \to +\infty} V(x) = +\infty$, $V'(x) > 0$, and $V''(x) < 0$.

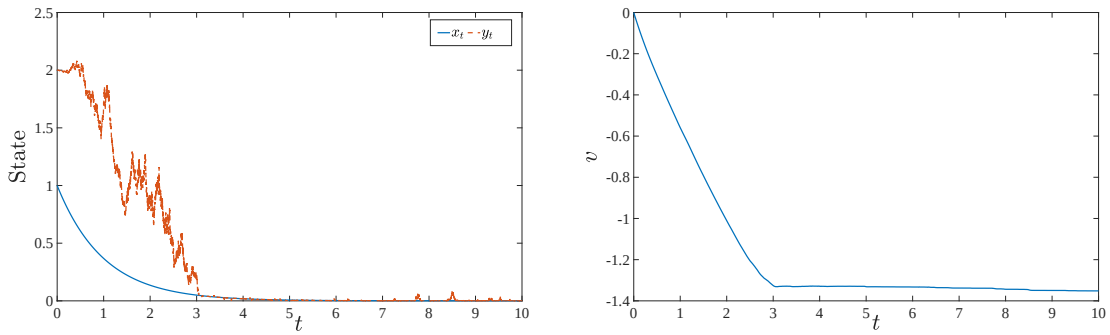

(a) (b)

Figure 8. (a) *Synchronized dynamics of x_t and y_t in system (6.3).* (b) *A failed case of parameter identification for the estimator v_t, where the identified parameter value converges to one different from the true value $\mu = -1$.*

Condition 6.2. The function g, defined on $(0, +\infty) \to (0, +\infty)$, satisfies $\lim_{x\to 0+} g(x)x = 0$.

Condition 6.3. The function $h(x) \triangleq -V''(x)g^2(x)x^2$, defined on $(0, +\infty) \to (0, +\infty)$, satisfies $\lim_{x\to 0+} h(x) = 0$ and

$$C_1 V'(x)x \le h(x) \le C_2 V'(x)x$$

for two positive numbers C_1 and C_2 and for all $x \ge 0$, where V is the function specified in Condition 6.1.

Example 6.4. Actually, the functions V, g, and h, which satisfy, respectively, Conditions 6.1, 6.2 and 6.3, can be concretely constructed. Examples include

$$g(x) = \begin{cases} \dfrac{1}{\sqrt{x}}, & 0 < x \le 1, \\ 1, & x > 1, \end{cases} \qquad h(x) = \begin{cases} x\mathrm{e}^{-x}, & 0 < x \le 1, \\ \dfrac{1}{\mathrm{e}}, & x > 1, \end{cases}$$

$$V(x) = \begin{cases} 1 - \mathrm{e}^{-x}, & 0 \le x \le 1, \\ \dfrac{1}{\mathrm{e}}(\ln x - 1) + 1, & x > 1, \end{cases}$$

which will be used in the examples below.

In the above setting and with the framework established in the preceding sections, we have the following theorem (a detailed proof and its preliminaries are provided in the appendix).

Theorem 6.5. *Suppose that Conditions 6.1–6.3 all hold. Any trajectory of system (6.2) eventually and almost surely synchronizes with the trajectory of system (6.1).*

Example 6.6. Consider $F(x,\mu)=\mu x$ and $\mu=-1$ in (6.1). The stochastically adaptive scheme is

$$\begin{cases} \mathrm{d}x=-x\mathrm{d}t, \\ \mathrm{d}y=vy\mathrm{d}t+kg(|y-x|)(y-x)\mathrm{d}B_t, \\ \mathrm{d}v=-yV'(|y-x|)\mathrm{sgn}(y-x)\mathrm{d}t, \\ \mathrm{d}k=h(|y-x|)\mathrm{d}t. \end{cases} \tag{6.3}$$

Numerical results are shown in Figure 8(a), where the states of $\boldsymbol{x}_t$ and $\boldsymbol{y}_t$ synchronize with each other, consistente with the analytical conclusion in Theorem 6.5. However, as shown in Figure 8(b), the estimator v_t does not converge to the true parameter value $\mu=-1$ but to -1.35 approximately, suggesting that successful parameter identification requires an additional condition besides Conditions 6.1–6.3.

Condition 6.7. For $i=1,2,\ldots,p$ and for any sequence $\{t_k\}_{k=1}^{+\infty}\to+\infty$, there exist m subsequences $\{t_k^s\}_{k=1}^{+\infty}\subset\{t_k\}_{k=1}^{+\infty}$ with $s=1,2,\ldots,m$ such that $\lim_{k\to+\infty}t_k^s=+\infty$ and $\lim_{k\to+\infty}\boldsymbol{x}(t_k^s)=\boldsymbol{x}_s$ for each s, and the matrix $\left\{f_{ij}(\boldsymbol{x}_s)\right\}_{j,s=1,2,\ldots,m}$ is nonsingular.

Theorem 6.8. *Suppose that Conditions 6.1–6.3 and Condition 6.7 all hold. Then, each estimator in system* (6.2) *satisfies* $\lim_{t\to+\infty}v_{ij}(t)=\mu_{ij}$ *almost surely in the set* $\left\{\sigma=+\infty\right\}$, *where* $\sigma\triangleq\inf\left\{t\geqslant 0:\|\boldsymbol{y}_t-\boldsymbol{x}_t\|=0\right\}$, *and* $\boldsymbol{x}_t$ *and* $\boldsymbol{y}_t$ *are the synchronized trajectories specified in Theorem 6.5.*

Theorem 6.8 presents a result on how to realize parameter estimation with the stochastically adaptive coupling scheme in some probability sense. The detailed proof of this theorem is included in the appendix. Here, Condition 6.7 assumed in this theorem was originally and similarly introduced in [37, 40].

Example 6.9. In order to illustrate Condition 6.7, we use the vector field $F(x,\mu)=\mu x+1$ with $\mu=-1$. The stochastically adaptive coupling scheme can be written as

$$\begin{cases} \mathrm{d}x=(-x+1)\mathrm{d}t, \\ \mathrm{d}y=(vy+1)\mathrm{d}t+kg(|y-x|)(y-x)\mathrm{d}B_t, \\ \mathrm{d}v=-yV'(|y-x|)\mathrm{sgn}(y-x)\mathrm{d}t, \\ \mathrm{d}k=h(|y-x|)\mathrm{d}t. \end{cases} \tag{6.4}$$

As shown in Figure 9, the estimator v tends to the true parameter value $\mu=-1$ while x_t and y_t are synchronized. The synchronization manifold $x=y=1$ makes the term μx a nonsingular constant, validating Condition 6.7. Note also that there are small fluctuations about the synchronization manifold and the true parameter value, due to the errors arising from the integration of the stochastic differential equations.

Example 6.10. We test parameter identification for the chaotic Lorenz system in Example 5.2. The stochastically adaptive coupling scheme is in

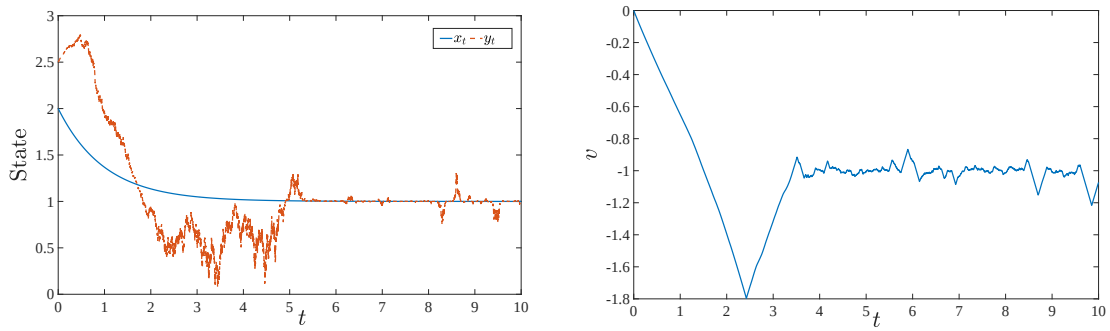

(a) (b)

Figure 9. (a) *Synchronized dynamics of x_t and y_t in system (6.4).* (b) *The estimator v_t converges to the true parameter value $\mu = -1$ with small fluctuations.*

$$
\begin{cases}
\mathrm{d}y_1 = v_1(y_2 - y_1)\mathrm{d}t + kg(\|\boldsymbol{y} - \boldsymbol{x}\|)(y_1 - x_1)\mathrm{d}B_t, \\
\mathrm{d}y_2 = (v_2 y_1 - y_1 y_3 - y_2)\mathrm{d}t + kg(\|\boldsymbol{y} - \boldsymbol{x}\|)(y_2 - x_2)\mathrm{d}B_t, \\
\mathrm{d}y_3 = (y_1 y_2 - v_3 y_3)\mathrm{d}t + kg(\|\boldsymbol{y} - \boldsymbol{x}\|)(y_3 - x_3)\mathrm{d}B_t, \\
\mathrm{d}v_1 = -(y_2 - y_1)V'(\|\boldsymbol{y} - \boldsymbol{x}\|)(y_1 - x_1)/\|\boldsymbol{y} - \boldsymbol{x}\|\mathrm{d}t, \\
\mathrm{d}v_2 = -y_1 V'(\|\boldsymbol{y} - \boldsymbol{x}\|)(y_2 - x_2)/\|\boldsymbol{y} - \boldsymbol{x}\|\mathrm{d}t, \\
\mathrm{d}v_3 = y_3 V'(\|\boldsymbol{y} - \boldsymbol{x}\|)(y_3 - x_3)/\|\boldsymbol{y} - \boldsymbol{x}\|\mathrm{d}t, \\
\mathrm{d}k = h(\|\boldsymbol{y} - \boldsymbol{x}\|)\mathrm{d}t.
\end{cases} \tag{6.5}
$$

As shown in Figure 10(a), the estimators $v_{1,2,3}$ approach the true values of parameters ($\sigma = 10$, $\rho = 28$, $\beta = 8/3$), indicating a successful case of identification. Note that the coupling gain k_t does not converge, due to the existence of a pseudosingularity, $\boldsymbol{y} - \boldsymbol{x} = \boldsymbol{0}$, in the denominators of the adaptive scheme (6.5). Indeed, the trajectory $\boldsymbol{y}_t$ changes its value in the direction of the driving trajectory $\boldsymbol{x}_t$, causing the discontinuity in the derivatives of v_{ij} in numerical computations. To illustrate this, we plot the logarithm of the synchronization error with t in Figure 10(b). It can be seen that, most of the time, the error is smaller than one. However, in the configuration of our adaptive scheme, the error sometimes fluctuates between the ceiling ($\mathrm{e}^4 \approx 54$) and the bottom (approximately at e^{-15}). These fluctuations result in the nonconvergence and monotonic increasing behavior of the coupling gain k_t in numerical simulations.

7. Concluding remarks.

We have developed a stochastically adaptive feedback scheme for stabilizing and synchronizing locally Lipschitzian systems in the sense of probability one. Compared with [36], there are three mathematical contributions: (a) an exact extension of the range of the power θ from $(0, 1)$ to the positive half axis, (b) a nontrivial generalization of the global Lipschitzian condition on the dynamical system's vector field to the locally Lipschitzian condition, and (c) an establishment of the criteria for guaranteeing stability and synchronization using noises of any finite dimensions. In addition to illustrating stabilization and synchronization with a number of representative examples, we have applied the control framework to the practical problem of parameter identification. All these demonstrate the

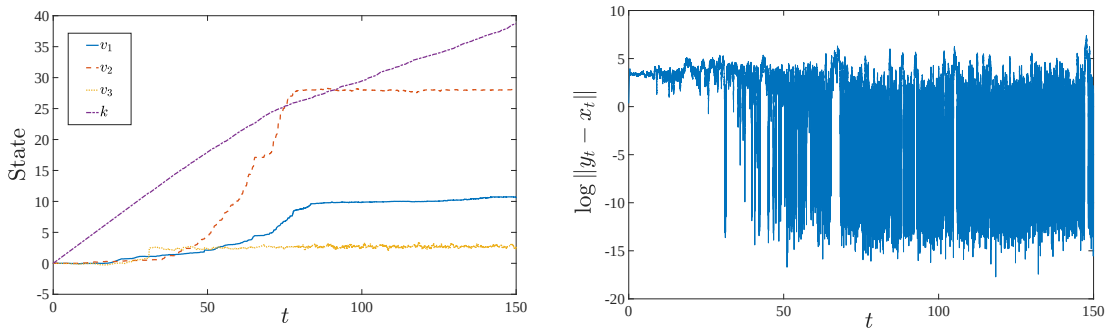

(a) (b)

Figure 10. (a) *Dynamics of the estimators and the coupling gain in system* (6.5). (b) *Time evolution of the logarithm of synchronization error* $\log\|\boldsymbol{y}_t - \boldsymbol{x}_t\|$.

effectiveness of our articulated stochastically adaptive control scheme and its general applicability to nonlinear and complex dynamical systems.

A number of open issues remain. For example, in physical and engineering applications it is desirable to develop mathematically justified, stochastically adaptive control schemes that optimize time and/or energy. Parameter identification based on data sets and data assimilation and the development of the underlying mathematical theory are another outstanding issue. A general mathematical framework for control and synchronization in dynamical systems with complex interacting structures, such as complex mutualistic networks in ecology [5, 17, 47, 34, 59, 11, 18, 30], is lacking at the present. The rigorous mathematical results and numerical demonstration in this paper provide a reasonable starting points for addressing these open problems that potentially have significant applications in many fields of science and engineering.

8. Appendix: Proofs of the theorems on parameter identification. To prove the main theorems on parameter identification, we need the following propositions (refer to [54]).

Proposition 8.1. *Suppose that Conditions 6.1–6.3 all hold. Then, for any given positive number* P*, there exists a positive number* K_P *such that* $g(x)^2x^2 \leq K_P h(x)$ *for all* $x \in [0, P]$.

Proposition 8.2. *Suppose that* $\boldsymbol{h}$ *is a uniformly continuous function defined on* $\mathbb{R}^+ \to \mathbb{R}^n$ *and the integral* $\int_0^{+\infty} \boldsymbol{h}(t)\mathrm{d}t$ *converges. Then,* $\lim_{t\to+\infty} \|\boldsymbol{h}(t)\| = 0$.

Proposition 8.3. *Suppose that* f *and* g *are two continuous functions defined on* $[0, +\infty)$. *Then, the following conclusions hold:*

(i) *If* g *is uniformly continuous with* $0 \leq g(t) \leq N$ *for some positive number* N*, then* $f(g(t))$ *is a uniformly continuous function.*

(ii) *If* $\lim_{t\to+\infty} g(t)$ *exists and is finite, then* g *is a uniformly continuous function on* $[0, +\infty)$.

(iii) *If* g *is bounded,* $\lim_{t\to+\infty} f(g(t)) = 0$*, and* $f(t) = 0$ *if and only if* $t = 0$*, then* $\lim_{t\to+\infty} g(t) = 0$.

Proof of Theorem 6.5. Define the following functional:

$$W_t = V(\|\boldsymbol{y}_t - \boldsymbol{x}_t\|) + \frac{1}{2}\sum_{i,j=1}^{N,m}(v_{ij} - \mu_{ij})^2 + \frac{k_t^3}{6} - \frac{Lk_t}{C_1}.$$

Applying Itô's formula to W yields

$$\begin{aligned} W_{t\wedge\sigma} = W_0 &\\ &+ \int_0^t \left[\frac{V'(\|\boldsymbol{y}_s - \boldsymbol{x}_s\|)}{\|\boldsymbol{y}_s - \boldsymbol{x}_s\|}\Big\langle \boldsymbol{y}_s - \boldsymbol{x}_s, \boldsymbol{F}(\boldsymbol{x}_s, \boldsymbol{\mu}) - \boldsymbol{F}(\boldsymbol{y}_s, \boldsymbol{\mu})\Big\rangle - \frac{L}{C_1}h(\|\boldsymbol{y}_s - \boldsymbol{x}_s\|)\right]\mathbf{1}_{s<\sigma}\mathrm{d}s \\ &+ \int_0^t k_s V'(\|\boldsymbol{y}_s - \boldsymbol{x}_s\|)g(\|\boldsymbol{y}_s - \boldsymbol{x}_s\|)\|\boldsymbol{y}_s - \boldsymbol{x}_s\|\mathbf{1}_{s<\sigma}\mathrm{d}Bs, \end{aligned}$$

where σ is the same as the one defined in Theorem 6.8. By Conditions 6.1–6.3, we obtain

$$\frac{V'(\|\boldsymbol{y}_s - \boldsymbol{x}_s\|)}{\|\boldsymbol{y}_s - \boldsymbol{x}_s\|}\Big\langle \boldsymbol{y}_s - \boldsymbol{x}_s, \boldsymbol{F}(\boldsymbol{x}_s, \boldsymbol{\mu}) - \boldsymbol{F}(\boldsymbol{y}_s, \boldsymbol{\mu})\Big\rangle - \frac{L}{C_1}h(\|\boldsymbol{y}_s - \boldsymbol{x}_s\|) \le 0.$$

According to the convergence lemma of the semimartingale, in the set $\{\sigma = +\infty\}$, $\lim_{t\to+\infty} W_t$ exists almost surely. Thus, k_t, $v_{ij}(t)$, and $V(\|\boldsymbol{y}_t - \boldsymbol{x}_t\|)$ are all bounded on $[0, +\infty)$. Because k_t is an increasing function, we have

$$\lim_{t\to+\infty} k_t = \int_0^{+\infty} h(\|\boldsymbol{y}_s - \boldsymbol{x}_s\|)\mathrm{d}s < +\infty.$$

On the other hand, we have that $\|\boldsymbol{y}_t - \boldsymbol{x}_t\|$ is bounded on $[0, +\infty)$ because $\lim_{x\to+\infty} V(x) = +\infty$ follows from Condition 6.1 which, with Proposition 8.1, implies

$$\int_0^{+\infty} k_s^2 g(\|\boldsymbol{y}_s - \boldsymbol{x}_s\|)^2\|\boldsymbol{y}_s - \boldsymbol{x}_s\|^2\mathrm{d}s < +\infty,$$

indicating that $\lim_{t\to+\infty}\int_0^t k_s g(\|\boldsymbol{y}_s - \boldsymbol{x}_s\|)(\boldsymbol{y}_s - \boldsymbol{x}_s)\mathrm{d}B_s$ exists and is finite almost surely in the set $\{\sigma = +\infty\}$. Since $\boldsymbol{x}_t$ is assumed to be bounded, $\boldsymbol{y}_t$ is bounded on $[0, +\infty)$ as well. Combining system (6.1) with its adaptive scheme (6.2) and Proposition 8.3(i), we conclude that $\boldsymbol{x}_t$ and $\boldsymbol{y}_t$ are both uniformly continuous functions on $[0, +\infty)$.

Proposition 8.3(ii) stipulates that $h(\|\boldsymbol{y}_t - \boldsymbol{x}_t\|)$ is a uniformly continuous function which, by Proposition 8.2, immediately results in $\lim_{t\to+\infty} h(\|\boldsymbol{y}_t - \boldsymbol{x}_t\|) = 0$. Therefore, by using Proposition 8.3(iii), we have that $\lim_{t\to+\infty}(\boldsymbol{y}_t - \boldsymbol{x}_t) = \mathbf{0}$. This completes the proof of stochastic synchronization. ∎

Proof of Theorem 6.8. First, we need to validate

$$\lim_{t\to+\infty} \boldsymbol{F}(\boldsymbol{x}_t, \boldsymbol{v}_t) - \boldsymbol{F}(\boldsymbol{x}_t, \boldsymbol{\mu}) = \mathbf{0} \tag{8.1}$$

almost surely. From Condition 6.1, we have $V'(\|\boldsymbol{y} - \boldsymbol{x}\|) \le V'(0)$, which indicates that for any trajectory in the set $\{\sigma = +\infty\}$, each derivative $\dot{v}_{ij}$ is bounded. This further implies uniform

continuity of each $v_{ij}(t)$. As a result, both $\boldsymbol{F}(\boldsymbol{y},\boldsymbol{v})$ and $\boldsymbol{F}(\boldsymbol{x},\boldsymbol{\mu})$ are uniformly continuous functions on $[0,+\infty)$. Moreover, it has been verified in the proof of Theorem 6.5 that both $\boldsymbol{y}_t-\boldsymbol{x}_t$ and $\int_0^t k_s g(\|\boldsymbol{y}_s-\boldsymbol{x}_s\|)(\boldsymbol{y}_s-\boldsymbol{x}_s)\mathrm{d}B_s$ converge finitely and almost surely as $t\to+\infty$. Thus, $\int_0^t[\boldsymbol{F}(\boldsymbol{y}_s,\boldsymbol{v}_s)-\boldsymbol{F}(\boldsymbol{x}_s,\boldsymbol{\mu}_s)]\,\mathrm{d}s$ converges finitely and almost surely as $t\to+\infty$ as well. This, together with the uniform continuity of $\boldsymbol{F}(\boldsymbol{y}_t,\boldsymbol{v}_t)-\boldsymbol{F}(\boldsymbol{x}_t,\boldsymbol{\mu})$ and Proposition 8.2, implies

$$\lim_{t\to+\infty}\boldsymbol{F}(\boldsymbol{y}_t,\boldsymbol{v}_t)-\boldsymbol{F}(\boldsymbol{x}_t,\boldsymbol{\mu})=\boldsymbol{0}$$

almost surely, proving consequently the validity of (8.1) by using $\lim_{t\to+\infty}(\boldsymbol{y}_t-\boldsymbol{x}_t)=\boldsymbol{0}$ almost surely, which follows from Theorem 6.5. Writing (8.1) componentwise yields

$$\lim_{t\to+\infty}\sum_{j=1}^{m}\big[v_{ij}(t)-\mu_{ij}\big]f_{ij}(\boldsymbol{x}_t)=0,\quad i=1,2,\ldots,p, \tag{8.2}$$

almost surely. We have that $v_{ij}(t)$ is bounded on $[0,+\infty)$ almost certainly in the set $\{\sigma=+\infty\}$. There then exists a sequence $\{t_k\}_{k=1}^{+\infty}\to+\infty$ such that $v_{ij}(t_k)\to v_{ij}^*$. Using Theorem 6.8, for each i, we have m subsequences $\{t_k^s\}_{k=1}^{+\infty}\subset\{t_k\}_{k=1}^{+\infty}$ $(s=1,2,\ldots,m)$ where, for each s, $\lim_{k\to+\infty}t_k^s=+\infty$, $\lim_{k\to+\infty}\boldsymbol{x}(t_k^s)=\boldsymbol{x}_s$, and the matrix $\{f_{ij}(\boldsymbol{x}_s)\}_{j,s=1,2,\ldots,m}$ is nonsingular. Setting $t=t_k^s$ in (8.2) and letting $k\to+\infty$, we obtain

$$\lim_{t\to+\infty}\sum_{j=1}^{m}\big(v_{ij}^*-\mu_{ij}\big)f_{ij}(\boldsymbol{x}_s)=0,\quad s=1,2,\ldots,m,$$

almost surely. Since the matrix $\{f_{ij}(\boldsymbol{x}_s)\}_{j,s=1,2,\ldots,m}$ is nonsingular, it follows that $v_{ij}^*=\mu_{ij}$, guaranteeing successful parameter identification almost surely in the set $\{\sigma=+\infty\}$. ∎

REFERENCES

[1] P. Achard and E. De Schutter, *Complex parameter landscape for a complex neuron model*, PLoS Comp. Biol., 2 (2006), e94.

[2] A. Ahlborn and U. Parlitz, *Stabilizing unstable steady states using multiple delay feedback control*, Phys. Rev. Lett., 93 (2004), 264101.

[3] J. A. Appleby, X. Mao, and A. Rodkina, *Stabilisation and destabilisation of nonlinear differential equations by noise*, IEEE Trans. Automat. Control, 53 (2008), pp. 683–691.

[4] L. Arnold, H. Crauel, and V. Wihstutz, *Stabilization of linear systems by noise*, SIAM J. Control. Optim, 21 (1983), pp. 451–461.

[5] J. Bascompte, P. Jordano, C. J. Melián, and J. M. Olesen, *The nested assembly of plant-animal mutualistic networks*, Proc. Natl. Acad. Sci. USA, 100 (2003), pp. 9383–9387.

[6] V. N. Belykh, I. V. Belykh, and M. Hasler, *Connection graph stability method for synchronized coupled chaotic systems*, Phys. D, 195 (2004), pp. 159–187.

[7] S. Boccaletti, C. Grebogi, Y.-C. Lai, H. Mancini, and D. Maza, *Control of chaos: Theory and applications*, Phys. Rep., 329 (2000), pp. 103–197.

[8] J. Cao and J. Lu, *Adaptive synchronization of neural networks with or without time-varying delay*, Chaos, 16 (2006), 013133.

[9] M. Chen, *Synchronization in time-varying networks: a matrix measure approach*, Phys. Rev. E, 76 (2007), 016104.

[10] F. Dai, S. Zhou, T. Peron, W. Lin, and P. Ji, *Interplay among inertia, time delay, and frustration on synchronization dynamics*, Phys. Rev. E, 98 (2018), 052218.

[11] V. Dakos and J. Bascompte, *Critical slowing down as early warning for the onset of collapse in mutualistic communities*, Proc. Natl. Acad. Sci. (USA), 111 (2014), pp. 17546–17551.
[12] R. FitzHugh, *Impulses and physiological states in theoretical models of nerve membrane*, Biophys. J., 1 (1961), pp. 445–466.
[13] H. Gao, X. Meng, T. Chen, and J. Lam, *Stabilization of networked control systems via dynamic output-feedback controllers*, SIAM J. Control Optim., 48 (2010), pp. 3643–3658.
[14] O. Golovneva, R. Jeter, I. Belykh, and M. Porfiri, *Windows of opportunity for synchronization in stochastically coupled maps*, Phys. D, 340 (2017), pp. 1–13.
[15] C. Grebogi and Y.-C. Lai, *Controlling chaos in high dimensions*, IEEE Trans. Cir. Sys., 44 (1997), pp. 971–975.
[16] R. O. Grigoriev, M. C. Cross, and H. G. Schuster, *Pinning control of spatiotemporal chaos*, Phys. Rev. Lett., 79 (1997), pp. 2795–2798.
[17] P. R. Guimaraes, P. Jordano, and J. N. Thompson, *Evolution and coevolution in mutualistic networks*, Ecol. Lett., 14 (2011), pp. 877–885.
[18] P. R. Guimaraes, M. M. Pires, P. Jordano, J. Bascompte, and J. N. Thompson, *Indirect effects drive coevolution in mutualistic networks*, Nature, 550 (2017), pp. 511–514.
[19] Y. Guo, W. Lin, and G. Chen, *Stability of switched systems on randomly switching durations with random interaction matrices*, IEEE Trans. Automat. Control., 63 (2018), pp. 21–36.
[20] Y. Guo, W. Lin, Y. Chen, and J. Wu, *Instability in time-delayed switched systems induced by fast and random switching*, J. Differantial Equations, 263 (2017), pp. 880–909.
[21] Y. Guo, W. Lin, and D. W. Ho, *Discrete-time systems with random switches: From systems stability to networks synchronization*, Chaos, 26 (2016), 033113.
[22] Y. Ha, Y. Guo, and W. Lin, *Non-bayesian social learning model with periodically switching structures*, Chaos, 31 (2021), 043137.
[23] M. Hasler, V. Belykh, and I. Belykh, *Dynamics of stochastically blinking systems. part* I: *Finite time properties*, SIAM J. Appl. Dyn. Syst., 12 (2013), pp. 1007–1030.
[24] M. Hasler, V. Belykh, and I. Belykh, *Dynamics of stochastically blinking systems. part* II: *Asymptotic properties*, SIAM J. Appl. Dyn. Syst., 12 (2013), pp. 1031–1084.
[25] J. L. Hindmarsh and R. M. Rose, *A model of neuronal bursting using three coupled first order differential equations*, Proc. Roy. Soc. London B Biol. Sci., 221 (1984), pp. 87–102.
[26] M. D. Holland and A. Hastings, *Strong effect of dispersal network structure on ecological dynamics*, Nature, 456 (2008), pp. 792–794.
[27] D. Huang, *Stabilizing near-nonhyperbolic chaotic systems with applications*, Phys. Rev. Lett., 93 (2004), 214101.
[28] L. Huang, *Stochastic stabilization and destabilization of nonlinear differential equations*, Systems Control Lett., 62 (2013), pp. 163–169.
[29] R. Jeter and I. Belykh, *Synchronization in on-off stochastic networks: Windows of opportunity*, IEEE Trans. Circuits Systems, 62 (2015), pp. 1260–1269.
[30] J. Jiang, Z.-G. Huang, T. P. Seager, W. Lin, C. Grebogi, A. Hastings, and Y.-C. Lai, *Predicting tipping points in mutualistic networks through dimension reduction*, Proc. Natl. Acad. Sci. USA, 115 (2018), pp. E639–E647.
[31] C. Kahl and H. Schurz, *Balanced Milstein methods for ordinary SDEs*, Monte Carlo Methods Appl., 12 (2006), pp. 143–170.
[32] R. Khasminskii, *Stochastic Stability of Differential Equations*, Stoch. Model. Appl. Probab. 66, Springer, New York, 2011.
[33] Y.-C. Lai and C. Grebogi, *Synchronization of chaotic trajectories using control*, Phys. Rev. E, 47 (1993), pp. 2357–2360.
[34] J. J. Lever, E. H. Nes, M. Scheffer, and J. Bascompte, *The sudden collapse of pollinator communities*, Ecol. Lett., 17 (2014), pp. 350–359.
[35] W. Lin, *Adaptive chaos control and synchronization in only locally Lipschitz systems*, Phys. Lett. A, 372 (2008), pp. 3195–3200.
[36] W. Lin, X. Chen, and S. Zhou, *Achieving control and synchronization merely through a stochastically adaptive feedback coupling*, Chaos, 27 (2017), 073110.

[37] W. Lin and H. Ma, *Failure of parameter identification based on adaptive synchronization techniques*, Phys. Rev. E, 75 (2007), 066212.
[38] R. Liptser and A. N. Shiryayer, *Theory of Martingales*, Springer, Berlin, 1989.
[39] E. N. Lorenz, *Deterministic nonperiodic flow*, J. Atmos. Sci., 20 (1963), pp. 130–141.
[40] H. Ma and W. Lin, *Nonlinear adaptive synchronization rule for identification of a large amount of parameters in dynamical models*, Phys. Lett. A, 374 (2009), pp. 161–168.
[41] H. Ma and W. Lin, *Realization of parameters identification in only locally lipschitzian dynamical systems with multiple types of time delays*, SIAM J. Control Optim., 51 (2013), pp. 3692–3721.
[42] X. Mao, *Stochastic stabilization and destabilization*, Systems Control Lett., 23 (1994), pp. 279–290.
[43] X. Mao, *Stochastic Differential Equations and Applications*, Elsevier, Amsterdam, 2007.
[44] X. Mao, G. G. Yin, and C. Yuan, *Stabilization and destabilization of hybrid systems of stochastic differential equations*, Automatica, 43 (2007), pp. 264–273.
[45] J. Nagumo, S. Arimoto, and S. Yoshizawa, *An active pulse transmission line simulating nerve axon*, Proc. IRE, 50 (1962), pp. 2061–2070.
[46] T. C. Newell, P. M. Alsing, A. Gavrielides, and V. Kovanis, *Synchronization of chaotic diode resonators by occasional proportional feedback*, Phys. Rev. Lett., 72 (1994), pp. 1647–1650.
[47] S. L. Nuismer, P. Jordano, and J. Bascompte, *Coevolution and the architecture of mutualistic networks*, Evolution, 67 (2013), pp. 338–354.
[48] E. Ott, C. Grebogi, and J. A. Yorke, *Controlling chaos*, Phys. Rev. Lett., 64 (1990), pp. 1196–1199.
[49] U. Parlitz, *Estimating model parameters from time series by autosynchronization*, Phys. Rev. Lett., 76 (1996), pp. 1232–1235.
[50] U. Parlitz, L. Junge, and L. Kocarev, *Synchronization-based parameter estimation from time series*, Phys. Rev. E, 54 (1996), pp. 6253–6259.
[51] L. M. Pecora and T. L. Carroll, *Synchronization in chaotic systems*, Phys. Rev. Lett., 64 (1990), pp. 821–824.
[52] M. Porfiri, D. J. Stilwell, E. M. Bollt, and J. D. Skufca, *Random talk: Random walk and synchronizability in a moving neighborhood network*, Phys. D, 224 (2006), pp. 102–113.
[53] P. E. Protter, *Stochastic Integration and Differential Equations*, Springer, Berlin, 2005.
[54] C. C. Pugh and C. Pugh, *Real Mathematical Analysis*, Undergrad. Texts Math. 2011, Springer, New York, 2002.
[55] K. Pyragas, *Continuous control of chaos by self-controlling feedback*, Phys. Lett. A, 170 (1992), pp. 421–428.
[56] K. Pyragas, *Control of chaos via extended delay feedback*, Phys. Lett. A, 206 (1995), pp. 323–330.
[57] I. Ratas and K. Pyragas, *Controlling synchrony in oscillatory networks via an act-and-wait algorithm*, Phys. Rev. E, 90 (2014), 032914.
[58] Y. Ren, W. Yin, and R. Sakthivel, *Stabilization of stochastic differential equations driven by G-Brownian motion with feedback control based on discrete-time state observation*, Automatica, 95 (2018), pp. 146–151.
[59] R. P. Rohr, S. Saavedra, and J. Bascompte, *On the structural stability of mutualistic systems*, Science, 345 (2014), 1253497.
[60] M. L. Rosenzweig and R. H. MacArthur, *Graphical representation and stability conditions of predator-prey interactions*, Am. Nat., 97 (1963), pp. 209–223.
[61] O. E. Rössler, *Equation for continuous chaos*, Phys. Lett. A, 57 (1976), pp. 397–398.
[62] W. Rudin, *Principles of Mathematical Analysis*, 3rd ed., McGraw-Hill, New York, 1976.
[63] J. S. Lawley and M. Reed, *Sensitivity to switching rates in stochastically switched ODEs*, Commun. Math. Sci., 12 (2014).
[64] A. A. Selivanov, J. Lehnert, T. Dahms, P. Hövel, A. L. Fradkov, and E. Schöll, *Adaptive synchronization in delay-coupled networks of Stuart-Landau oscillators*, Phys. Rev. E, 85 (2012), 016201.
[65] F. Sorrentino and E. Ott, *Adaptive synchronization of dynamics on evolving complex networks*, Phys. Rev. Lett., 100 (2008), 114101.
[66] Y.-Z. Sun, S.-Y. Leng, Y.-C. Lai, C. Grebogi, and W. Lin, *Closed-loop control of complex networks: A trade-off between time and energy*, Phys. Rev. Lett., 119 (2017), 198301.

[67] Z. Sun, W. Zhu, G. Si, Y. Ge, and Y. Zhang, *Adaptive synchronization design for uncertain chaotic systems in the presence of unknown system parameters: A revisit*, Nonlinear Dyn., 72 (2013), pp. 729–749.
[68] J. M. T. Thompson and H. B. Stewart, *Nonlinear Dynamics and Chaos*, 2nd ed., John Wiley & Sons, New York, 2002.
[69] W. Van Geit, P. Achard, and E. De Schutter, *Neurofitter: A parameter tuning package for a wide range of electrophysiological neuron models*, BMC Neurosci., 8 (2007), p. P5.
[70] W. Walter, *Differential and Integral Inequalities*, Springer, Berlin, 1970.
[71] X. F. Wang and G. Chen, *Pinning control of scale-free dynamical networks*, Phys. A, 310 (2002), pp. 521–531.
[72] X.-J. Wang, *Genesis of bursting oscillations in the Hindmarsh-Rose model and homoclinicity to a chaotic saddle*, Phys. D, 62 (1993), pp. 263–274.
[73] A. R. Willms, D. J. Baro, R. M. Harris-Warrick, and J. Guckenheimer, *An improved parameter estimation method for Hodgkin-Huxley models*, J. Comp. Neurosci., 6 (1999), pp. 145–168.
[74] Z. Wu, *Stability criteria of random nonlinear systems and their applications*, IEEE Trans. Automat. Control, 60 (2014), pp. 1038–1049.
[75] Z. Wu, M. Cui, P. Shi, and H. R. Karimi, *Stability of stochastic nonlinear systems with state-dependent switching*, IEEE Trans. Automat. Control, 58 (2013), pp. 1904–1918.
[76] W. Xia and J. Cao, *Pinning synchronization of delayed dynamical networks via periodically intermittent control*, Chaos, 19 (2009), 013120.
[77] N. Yadaiah, B. L. Deekshatulu, L. Sivakumar, and V. S. H. Rao, *Neural network algorithm for parameter identification of dynamical systems involving time delays*, Appl. Soft Comp., 7 (2007), pp. 1084–1091.
[78] D. Yu and U. Parlitz, *Estimating parameters by autosynchronization with dynamics restrictions*, Phys. Rev. E, 77 (2008), 066221.
[79] W. Yu, G. Chen, J. Cao, J. Lü, and U. Parlitz, *Parameter identification of dynamical systems from time series*, Phys. Rev. E, 75 (2007), 067201.
[80] W. Yu, G. Chen, J. Lu, and J. Kurths, *Synchronization via pinning control on general complex networks*, SIAM J. Control Optim., 51 (2013), pp. 1395–1416.
[81] B. Zhang, *Stochastic differential equations and their applications*, in Handbook of Stochastic Analysis and Applications, CRC Press, Boca Raton, FL, 1976, pp. 159–235.
[82] J. Zhou, J. Lu, and J. Lü, *Adaptive pinning synchronization of a general complex dynamical network*, in Proceedings of the IEEE International Symposium on Circuits and Systems, 2007, pp. 2494–2497.
[83] S. Zhou, Y. Guo, M. Liu, Y.-C. Lai, and W. Lin, *Random temporal connections promote network synchronization*, Phys. Rev. E, 100 (2019), 032302.
[84] S. Zhou, P. Ji, Q. Zhou, J. Feng, J. Kurths, and W. Lin, *Adaptive elimination of synchronization in coupled oscillator*, New J. Phys., 19 (2017), 083004.
[85] S. Zhou and W. Lin, *Eliminating synchronization of coupled neurons adaptively by using feedback coupling with heterogeneous delays*, Chaos, 31 (2021), 023114.
[86] S. Zhu, J. Zhou, G. Chen, and J.-a. Lu, *Estimating the region of attraction on a complex dynamical network*, SIAM J. Control Optim., 57 (2019), pp. 1189–1208.
[87] B. Øksendal, *Stochastic Differential Equations*, Springer, Berlin, 2003.